Arabian Journal of Chemistry (2023) **16**, 104818

King Saud University

Arabian Journal of Chemistry

www.ksu.edu.sa
www.sciencedirect.com

ORIGINAL ARTICLE

Implementation of Amorphous Mesoporous Silica Nanoparticles to formulate a novel water-based drilling fluid

Vahid Zarei [a,b,*], Hossein Yavari [c,d], Alireza Nasiri [c,d], Mojtaba Mirzaasadi [e,f], Afshin Davarpanah [a]

[a] *Department of Petroleum Engineering, Faculty of Petroleum and Chemical Engineering, Science and Research Branch, Islamic Azad University (IAU), Tehran, Iran*
[b] *Department of Materials Science and Engineering, School of Engineering, Shiraz University, Zand Ave., Shiraz, Iran*
[c] *Department of Petroleum Engineering, Amirkabir University of Technology, Tehran 15875-4413, Iran*
[d] *Research and Development Department of Upstream Petroleum Industry Research Center, Petroleum Engineering Division, Research Institute of Petroleum Industry (RIPI), Tehran 14857-33111, Iran*
[e] *Mapna Drilling Company (MDCo), Gandhi St., Vanak Sq., Tehran 1517935111, Iran*
[f] *Department of Chemical Engineering, Laval University, Québec G1V 0A6, Canada*

Received 13 December 2022; accepted 15 March 2023
Available online 24 March 2023

KEYWORDS

Drilling mud;
Shale instability;
Sol–gel method;
Amorphous Mesoporous Silica Nanoparticles;
Rheological properties;
Thermal stability

Abstract One of the significant problems of drilling with water-based muds in oil and gas wells is the instability in the Shale Formations. Conventional additives cannot plug nanometer-sized pore throats of Shale. Today, Nanotechnology is used to improve the performance of water-based muds. Adding some Nanoparticles with unique properties to drilling fluids has remarkably improved the mud's properties. Therefore, this study synthesized Amorphous Mesoporous Silica Nanoparticles (AMSN) with heightened purity and suitable Special Surface Area (SSA) using the sol–gel method. Then AMSN was employed in an eco-friendly water-based mud to investigate the effect on rheological properties, filtration, thermal stability, and Shale recovery.

Several analyses were conducted on AMSN synthesized by TEM, FESEM, EDX, DLS, XRF, XRD, BJH, and BET. According to the results, AMSN has an amorphous phase, and its purity, SSA, and total pore volume stand at 98.99%, 226.13 ($m^2.g^{-1}$), and 1.0539 ($m^3.g^{-1}$). Under two conditions, the AMSN was incorporated into the water-based drilling fluid at four concentrations: 0.1, 0.5, 1, and 2% W/W. The primary condition is Before Hot Rolling (BHR), conducted at a

* Corresponding author.
E-mail addresses: vahid.zarei@srbiau.ac.ir, vahid.zarei@hafez.shirazu.ac.ir (V. Zarei).
Peer review under responsibility of King Saud University.

Production and hosting by Elsevier

https://doi.org/10.1016/j.arabjc.2023.104818

Nomenclature

AHR	After Hot Rolling.
AMSN	Amorphous Mesoporous Silica Nanoparticles.
API	American Petroleum Institute.
AV	Apparent viscosity, cP.
BHR	Before Hot Rolling.
FL	Fluid Loss, mL.
Gs	gel strength, lbf/100ft^2.
MW	Mud weight, pcf.
OBM	Oil based Mud.
PV	Plastic viscosity, cP.
Rpm	rotation per minute.
S.G.	Specific Gravity
TEOS	Tetraethyl Orthosilicate.
WBM	Water-Based Mud.
YP	Yield point, lbf/100ft^2.

temperature of 43.3 °C. A second trial was conducted after hot rolling (AHR) at simulated downhole temperatures of 121.1 °C and 148.8 °C, respectively. In both conditions, the results indicate that the ideal concentration of AMSN is 0.1% by weight and improves the rheological properties, thermal stability, and Shale recovery. Comparatively to base mud, an optimal concentration of AMSN can increase apparent viscosity by 12.5% and reduce fluid loss by 55% in AHR conditions.

1. Introduction

In recent decades, the global energy demand has increased significantly. Accordingly, oil and gas are the main sources of energy when compared to other sources. The production of energy from renewable energy sources such as biomass, geothermal, wind, solar, and nuclear sources is more expensive than conventional fossil fuels (Oseh et al., 2019; Karakosta et al., 2021; Dhinesh and Annamalai, 2018). In the past few decades, new technologies, and oil and gas exploration have improved, and deeper formations are being drilled (Nanthagopal et al., 2019; Annamalai et al., 2016). To ensure an economical and successful drilling operation, it is therefore vital to improve the drilling fluids to overcome the harsh conditions associated with deep Formation to achieve a successful drilling operation (Bizhani et al., 2016).

Nanomaterials have been extensively applied to the oil and gas industry in several fields including well stimulation, enhanced oil recovery (EOR), and drilling mud formulations in recent research (Harati et al., 2020; Singh et al., 2018; Patidar et al., 2021; Jafariesfad et al., 2016; Bashir Abdullahi et al., 2019). Several researchers have successfully used nanomaterials as additives to improve the rheological properties of drilling muds as well as to improve the filtration of drilling fluids (Zarei and Nasiri, 2021; Rafati et al., 2018; Bayat and Shams, 2019). Additionally, nanomaterials have been successfully used to improve Shale recovery, thermal stability, heat transfer, cutting transport, and hole cleaning, as well as reducing torque and drag, minimizing stuck pipes, maintaining wellbore stability, and reducing Formation damage (Abbas et al., 2021; Jain et al., 2015; Mao et al., 2015; Shojaei and Ghazanfari, 2022; Xu et al., 2018).

Several literature studies have revealed that Nanoparticles such as zinc oxide (ZnO), copper oxide (CuO), iron oxide (Fe_2O_3), aluminum oxide (Al_2O_3), graphene oxide (GO), carbon nanotubes (CNT), titanium dioxide (TiO_2), zirconium oxide (ZrO_2), and silicon oxide (SiO_2) have been employed to improve the properties of drilling fluids (Sajjadian et al., 2020; Kök and Bal, 2019; Bayat et al., 2018; Sadegh Hassani et al., 2016). A nanomaterial that is extensively used in the preparation of drilling mud is Nano Silica, which is used in many drilling mud formulations. (Srivatsa and Ziaja, 2011; Vryzas et al., 2015). Nano Silica is one of the additives that can be used in the design of environmentally friendly water-based muds (Yang et al., 2017). Many techniques can be used in the production of Nano Silica, such as the Plasma method, the Microwave radiation method, and the Sol-gel method (William et al., 2014; Ramesh, 2009). Zarei et al, (2021), and Mirzaasadi et al., (2021), proposed a new way to extract Nano Silica from agricultural waste materials such as rice husks, and this method could be performed quickly and cheaply (Zarei et al., 2021), (Mirzaasadi et al., 2021).

The literature has found that low concentrations of Nano Silica can improve the rheological and filtration properties of WBM (Salih et al., 2016). Esfandyari et al. (2021) investigated the effect of Nano Silica (SiO_2) and titanium dioxide (TiO_2) on the rheological properties of water-based polymeric mud and the efficiency of filtration at 25, 50, and 75 °C with varying concentrations ranging from 0.01 to 0.5 wt %. These nanomaterials were found to be capable of increasing the yield point and the gel strength and reducing the plastic viscosity and filtration (Esfandyari Bayat et al., 2021).

Oseh et al. (2020) formulated a new WBM by Nanocomposites which is known as (3-Aminopropyl) Triethoxysilane modified polypropylene-Silica nanocomposite (PP-SiO_2 NC-NH_2) not only to lift cuttings out of the annulus during drilling operation but also for enhancing the rheological and filtration properties of the drilling muds (Oseh et al., 2020). A study carried out by Mikhienkova et al. (2022) found that Silica Nanoparticles were able to improve a variety of rheological properties in the oil-based drilling fluid. This included friction, filtration, and colloidal stability (Mikhienkova et al., 2022). Other research by Katende et al. (2019) shows that Silica Nanoparticles can improve the rheological and filtration performance of OBM and WBM systems at high temperatures (Katende et al., 2019).

Researchers have also used Silica Nanoparticles to clean and prevent gas hydrate in gas Formation. Elochukwu et al. (2017) proposed a new approach to improve water-based muds' cutting transport and carrying capacity using Nano Silica particles in both conditions; low pressure and low temperature (LPLT) and high pressure and high temperature (HPHT). Furthermore, this study indicated that adding Nano Silica can create a thin, low-permeability filter cake (Elochukwu et al., 2017). Zhao et al. (2021) tested five types of Nanoparticles suspended in aqueous NaCl solutions to control quartz and kaolinite fine migration. The findings revealed that Nanoparticles could effectively absorb and fix fine particles (Zhao et al., 2021). A study conducted by Prakash et al. (2021) evaluated the effect of Silica Nanoparticles on Grewia Optivia fiber powder (GOFP), as an environmentally friendly additive, in water-based drilling fluids. Based on their results, the 5% GOFP + 4% Silica Nanoparticles mixture reduced LPLT and HPHT fluid losses by 74.03 and 78.12%, respectively, compared to base mud

(Prakash et al., 2021). The application of Silica Nanoparticles to reduce Formation damage has been demonstrated by Shojaei et al. (2022) through combined experimental and numerical methods. In both water and oil-saturated porous media, samples with 0.2 wt% hydrophobic Nano Silica performed best, with returning permeability of 68.4% (Shojaei and Ghazanfari, 2022). A flow loop system with 0 to 150 rotational per minute was used by Boyou et al. (2019) to study how Silica Nanoparticles influenced hole cleaning. Results showed that Silica Nanoparticles increased the colloidal interaction with cuttings and enhanced hole-cleaning efficiency by up to 44% (Boyou et al., 2019).

The use of Silica Nanoparticles in water-based mud to enhance hole-cleaning properties has been reported by Gbadamosi et al. (2019). It examined how flow rate, Nano Silica concentration, and cutting size affect hole cleaning. According to experimental results, Silica Nanoparticle concentration and flow rate are directly related to wellbore cleaning (Gbadamosi et al., 2019).

Chaturvedi et al. (2021) utilized Silica Nanofluids as additives in water-based drilling muds for drilling gas hydrate reservoirs. Researchers found that Silica Nanofluids in drilling muds helped to stabilize absorbed gas bubbles and minimize gas blowouts during drilling (Chaturvedi et al., 2021).

This research was designed to assess the performance of AMSN on a polymeric-limestone WBM at 43.3, 121.1, and 148.8 °C. Moreover, the influences of AMSN were also appraised to find the optimum concentration. For this goal, a polymer-based limestone WBM utilized to drill the reservoir section of some Iranian oil fields was formulated in the laboratory, and then AMSN was added at different concentrations ranging from 0.1 to 2 % wt. After that, the rheological and filtration properties of the drilling fluid and Shale recovery were studied.

2. Materials and methods

2.1. Materials

In this study, The Shale cuttings used were obtained from one of the oil fields in southern Iran. Other materials are employed; sulfuric acid (H_2SO_4 = 98%), caustic soda (NaOH = 98%), soda ash (Na_2CO_3 = 98%), Tetra Ethyl Orthosilicate (TEOS = 99.9%), ammonium hydroxide (NH_4OH = 28%), ethanol (C_2H_5OH = 99.9%), were procured from Merck Company (Germany). All reagents were used without further purification.

2.2. Synthesis AMSN

This study synthesized Silica Nanoparticles with amorphous and porous structures using the Sol–gel method and precursor materials of Silica alkoxide (TEOS). The synthesis process is based on TEOS hydrolysis and polymerization, according to Eq. (1) and Fig. 1., in an environment containing ethanol and distilled water. In this process, sulfuric acid is used as the acid reactant, and ammonium hydroxide is used as the alkaline reactant (Rahman et al., 2008; Vasconcelos et al., 2002; Jal et al., 2004). A hydrolysis reaction is performed by placing TEOS in ethanol and water to produce an intermediate product called a single-stage hydrolyses monomer with the formula $Si(OC_2H_5)_3OH$ (Folgar et al., 2007). According to Eq. (2) and Fig. 2, an intermediate product based on the reaction polymerization produced water, known as the water condensation reaction. With the reaction of the products of the previous stage and single-stage hydrolyses monomers based on the reaction Eq. (3) and Fig. 3, another polymerization has been done. This step is known as the Alcohol condensation reaction due to the production of alcohol (Rahman and Padavettan, 2012).

The presence of sulfuric acid in the synthesis of Nano Silica as a catalyst has increased the speed of TEOS hydrolysis and Polycondensation reactions and raised the production efficiency of Nanoparticles (Rahman et al., 2007, Rahman et al., 2006).

To synthesize, first, 200 cc of ethanol was placed on a stirrer, and 25 cc of TEOS was added to it and mixed for 15 min. Then 50 cc of distilled water was added to the prepared solution. Subsequently, sulfuric acid 10% was added to the previous formula to reduce pH (approximately 2.5 ~ 3). The mixing process was performed at ambient temperature for 1 h to obtain Sol. After 1 h, ammonium hydroxide was added to increase pH (approximately 9.5 ~ 10), and the mixing was performed to obtain a Gel-like product. Afterward, the Gel was washed with distilled water several times using a vacuum pump and the Buchner funnels. Then the Gel is placed in the freezer at −70 °C for 24 h. The drying process is performed under a vigorous vacuum condition (Pan et al., 2017).

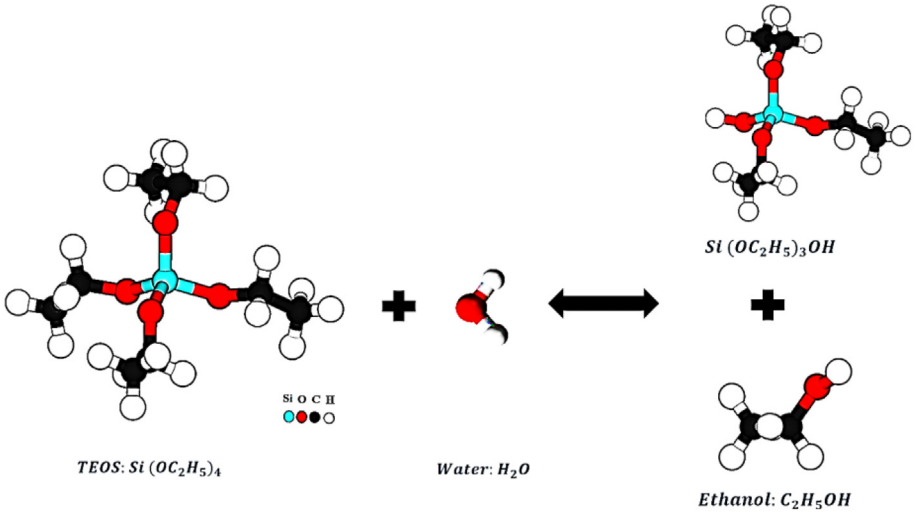

Fig. 1 Stepwise of Hydrolyses TEOS.

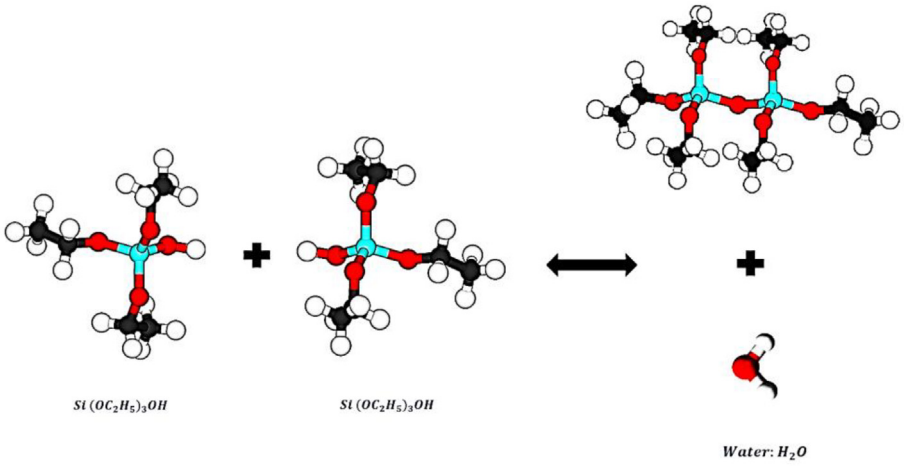

Fig. 2 Stepwise reaction water condensation.

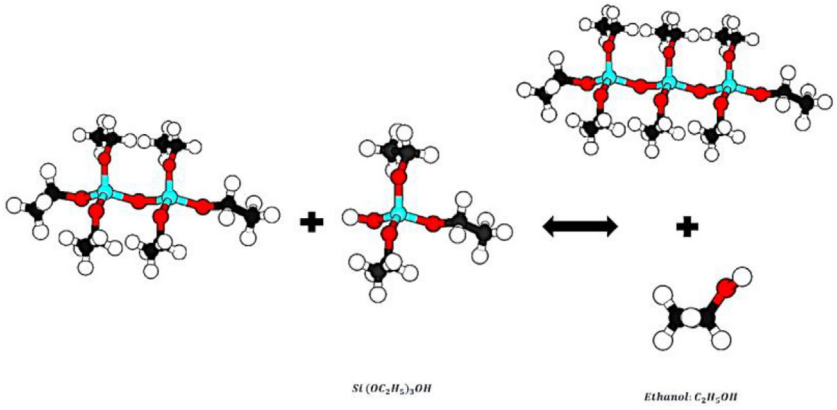

Fig. 3 Stepwise of reaction alcohol condensation.

$$Si(OC_2H_5)_4 + H_2O \leftrightarrow Si(OC_2H_5)_3OH + C_2H_5OH$$
$$\equiv Si - O - C_2\ H_5\ +\ H_2\ O\ \leftrightarrow\equiv Si - O - H \equiv +\ C_2H_5OH \quad (1)$$

$$Si(OC_2H_5)_3OH + Si(OC_2H_5)_3OH \leftrightarrow\equiv Si - O - Si \equiv +H_2O$$
$$\equiv Si - O - H + H - O - Si \equiv\leftrightarrow\equiv Si - O - Si \equiv +H_2O \quad (2)$$

$$Si(OC_2H_5)_4 + Si(OC_2H_5)_3OH \leftrightarrow\equiv Si - O - Si \equiv +C_2H_5OH$$
$$\equiv Si - O - C_2H_5 + H - O - Si \equiv\leftrightarrow\equiv Si - O - Si \equiv +C_2H_5OH \quad (3)$$

2.3. Drilling fluid preparation

The methodologies for preparing muds and measuring the properties are according to a local laboratory experimental work standard called NISOC and recommended practice for field testing Water-Based drilling fluid (API RP 13B-1, 2009).

Nanoparticles must be thoroughly dispersed to work optimally (Barroso et al., 2018; Addagalla et al., 2018). Dispersion of Nano Silica particles is stabilized in drilling muds using polymers such as Starch LV and PAC- LV (McElfresh et al., 2012; Ma et al., 2018; Rimer et al., 2007). The pH of the mud is then maintained above nine to ensure that the dispersion of Nano Silica and polymers is stabilized. A high pH condition guarantees the dispersion of Nano Silica particles. Silica Nanoparticles can acquire an anionic charge when dispersed at a high pH. Silica Nanoparticles that have been charged on their surfaces become self-repulsive, causing them to disperse well. Experiments indicate that it takes longer for Silica Nanoparticles to settle in a water-based environment with a high pH than in deionized water. In addition, when Nanoparticles settle in a high pH environment, their height is greater than when they settle in deionized water. Because Nanoparticle surface charge enhances their dispersion by inhibiting them from approaching and adhering to one another (Katende et al., 2019). The designed WBM formulation is tabulated in Table 1.

In order to prepare the base drilling fluid sample, 0.5 gr of Soda Ash was added to 350 mL of Salt Saturated Water (SSW) to reduce calcium ions' water hardness and contamination. SSW was made by dissolving 355 g of sodium chloride salt in 1000 mL of water at 25 °C. After it, 0.2 gr of Caustic Soda was added to set the pH of the mud in the range of 9 to 9.5 $\mp$ 0.5. At continuing, samples were mixed by a 5-spindle multimixer at 11500 rpm for 5 min. At the end of 5 min, the AMSN

Table 1 Designed water-based mud formulation for 1.36 S.G. mud weight.

No.	Additive	Function	Composition
1	**Salt Saturated Water (NaCl) (355 gr NaCl in 1000 mL freshwater)**	Base fluid	350 mL
2	**Soda Ash (Na_2CO_3)**	Treating water contamination	0.5 gr
3	**Caustic Soda (NaOH)**	Controlling PH	0.2 gr
4	**Starch LV**	Viscosifiers and fluid loss controller	6 gr
5	**PAC LV**	Fluid loss controller	6 gr
6	**Limestone**	Weighting agent	113 gr

Table 2 Result of rheological properties base drilling fluids and drilling fluids containing AMSN.

		Mud Properties																		
		θ_1	**θ_2**	**θ_3**	**θ_6**	**θ_{10}**	**θ_{20}**	**θ_{30}**	**θ_{60}**	**θ_{100}**	**θ_{200}**	**θ_{300}**	**θ_{600}**	**GEL $\frac{10sec}{10min}$**	**AV**	**PV**	**YP**	**T**	**FL**	**pH**
	unit	–	–	–	–	–	–	–	–	–	–	–	–	$\frac{lb_f}{100ft^2}$	cP	cP	$\frac{lb_f}{100ft^2}$	°C	mL	–
Mud Base (MB)	BHR	2	2.5	3	4	6	7	9	13	16	24	31	47	3/4	23.5	16	15	43.3	6	9.5
	AHR	0	0.5	1	1.5	2	3	4	6	9	15	19	32	1/1.5	16	13	6	60	6.8	8.74
MB + **AMSN** 0.1% W/W	BHR	2	2.5	3	4	6	7	9	13	17	25	32	49	3/4	24.5	17	15	43.3	5	9.4
	AHR	0.5	1	1.5	2	2.5	4	5	7	10	16	22	36	1.5/2	18	14	8	60	3	8.61
MB + **AMSN** 0.5% W/W	BHR	2.5	3	4	5	7	9	11	16	21	30	38	58	4/5	29	20	18	43.3	10	8.9
	AHR	4	5	6	7	8	11	13	19	24	34	42	63	6/7	31.5	21	21	60	11	7.3
MB + **AMSN** 1% W/W	BHR	6	7	8	10	12	15	17	22	28	38	47	68	8/10	34	21	26	43.3	18	8.6
	AHR	10	11	12	14	15	19	21	27	33	45	55	80	12/14	40	25	30	60	16.5	7.12
MB + **AMSN** 2% W/W	BHR	21	23	24	26	28	31	33	38	43	54	63	88	24/26	44	25	38	43.3	15	8.5
	AHR	26	28	29	30	32	33	36	42	48	62	74	105	29/30	52.5	31	43	60	14	7.05

Table 3 Shale recovery and rheological properties of mud and 20 gr Shale at 121.1 ℃ for 8 h.

		Mud Properties																			
		θ_1	**θ_2**	**θ_3**	**θ_6**	**θ_{10}**	**θ_{20}**	**θ_{30}**	**θ_{60}**	**θ_{100}**	**θ_{200}**	**θ_{300}**	**θ_{600}**	**GEL $\frac{10sec}{10min}$**	**AV**	**PV**	**YP**	**T**	**FL**	**pH**	**Shale Rec**
	unit	–	–	–	–	–	–	–	–	–	–	–	–	$\frac{lb_f}{100ft^2}$	cP	cP	$\frac{lb_f}{100ft^2}$	°C	mL	–	%
Mud Base (MB)	BHR	2	2.5	3	4	6	7	9	13	16	24	31	47	3/4	23.5	16	15	43.3	6	9.5	–
	AHR	0.5	1	1.5	2.5	3	4	5	8	12	19	24	38	1.5/2.5	19	14	10	60	5.15	8.6	93
MB + **AMSN** 0.1% W/W	BHR	2	2.5	3	4	6	7	9	13	17	25	32	49	3/4	24.5	17	15	43.3	5	9.4	–
	AHR	1	1.5	2	3	4	4.5	6	9	13	20	26	41	2/3	20.5	15	11	60	3.1	7.9	97

powder is added, and the solution is mixed for 10 min. Then 6 gr of starch LV was added and mixed for 20 min to increase the viscosity. Furthermore, to enhance the filtration and rheological properties of the prepared mud in higher temperatures, 6 gr of PAC-LV were gently added and mixed for 20 min. Finally, 113 gr of limestone was added, and it was mixed for 10 min to increase the density of the prepared mud to 85 Pounds Per Cubic Foot (pcf), which is equivalent to 1362.2 Kg per cubic meter (Kg/m^3).

2.4. Assessing mud properties

The effect of AMSN in the WBM at four concentrations of 0.1, 0.5, 1, and 2% w/w were investigated. Experiments were

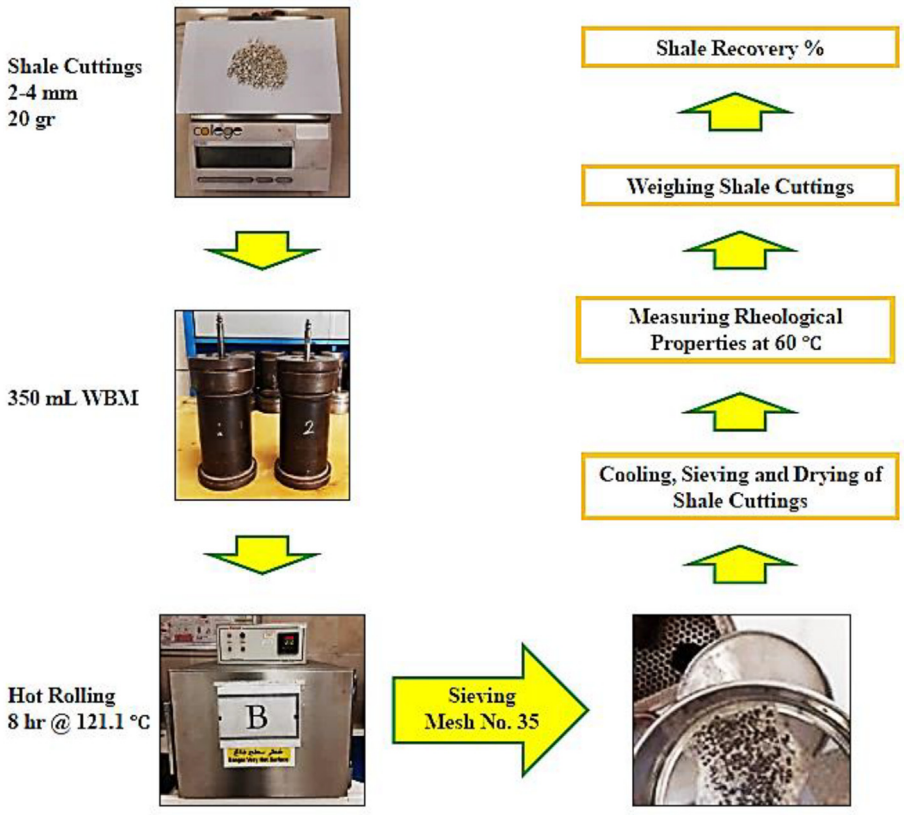

Fig. 4 Shale recovery test.

performed to determine the influence of AMSN on changes in rheology, pH, and fluid loss of the base mud. Two experiments were performed to determine changes in the base mud properties due to adding AMSN.

In the first experiment, the mud properties were measured after adding AMSN before heating and rolling. In the second experiment, the mud properties were measured after heating and rolling for four hours at 121.1 °C to simulate downhole conditions during the drilling operation (see Table 2). The essential rheological properties of the mud samples, including shear stress vs. shear rate, apparent viscosity (AV) in cP, plastic viscosity (PV) in cP, yield point (YP) in $\boldsymbol{lb_f/100ft^2}$, and gel strength (GS) in $\boldsymbol{lb_f/100ft^2}$, were measured using a V-G meter, model Chan 35. To measure these properties shear stress values of the prepared mud samples at 1, 2, 3, 6, 10, 20, 30, 60, 100, 200, 300, and 600 rpm were measured using the V-G meter. AV, PV, and YP were calculated using Eq. (4), Eq. (5) and Eq. (6). (Mirzaasadi et al., 2021; Pakdaman et al., 2019; Novara et al., 2021),

$$AV = \frac{\theta_{600}}{2} \tag{4}$$

$$PV = \theta_{600} - \theta_{300} \tag{5}$$

$$YP = \theta_{300} - PV \tag{6}$$

Gel strength measurement tests were done at a shear rate of 3 rpm to measure the mud's shear stresses after 10 s and 10 min of rest. This process is done according to the API standards procedure. Filtrate loss tests were done at 77 °F (25 °C) and 100 psi using a six-unit low-pressure, low-temperature filter press equipment. The mud's filtration volume was measured in 30 min (Mirzaasadi et al., 2021; Esfandyari Bayat et al., 2021). To determine the acidity of the mud at ambient temperature, a pH meter model WTW 323 was used.

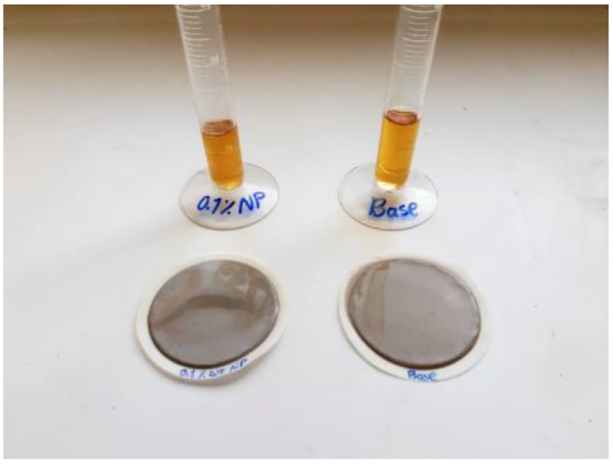

Fig. 5 Mud cake and fluid loss after hot rolling test; right to left: a) Base mud. b) 0.1% W/W AMSN.

2.5. Shale dispersion test

According to Table 2, the concentration of 0.1 w/w of AMSN is the optimum concentration because it improves the rheolog-

Table 4 The rheological properties of base drilling fluid and Shale recovery at 148.8 °C.

		Mud Properties																		
		θ_1	θ_2	θ_3	θ_6	θ_{10}	θ_{20}	θ_{30}	θ_{60}	θ_{100}	θ_{200}	θ_{300}	θ_{600}	GEL $\frac{10sec}{10min}$	AV	PV	YP	T	FL	pH	Shale Rec
	unit	–	–	–	–	–	–	–	–	–	–	–	–	$\frac{Ib_f}{100ft^2}$	cP	cP	$\frac{Ib_f}{100ft^2}$	°C	mL	–	%
Mud Base (MB)	BHR	2	2.5	3	4	6	7	9	13	16	24	31	47	3/4	23.5	16	15	43.3	6	9.5	–
	AHR	1	1.5	2	2.5	3.5	5	6	7	9	14	18	29	2/2.5	14.5	11	7	60	17	7.9	90
MB	BHR	2	2.5	3	4	6	7	9	13	17	25	32	49	3/4	24.5	17	15	43.3	5	9.4	–
+ **AMSN** 0.1% W/W	AHR	1.5	2	2.5	3	4	5.5	7	8	10	15	19	31	2.5/3	15.5	12	7	60	14	7.1	93

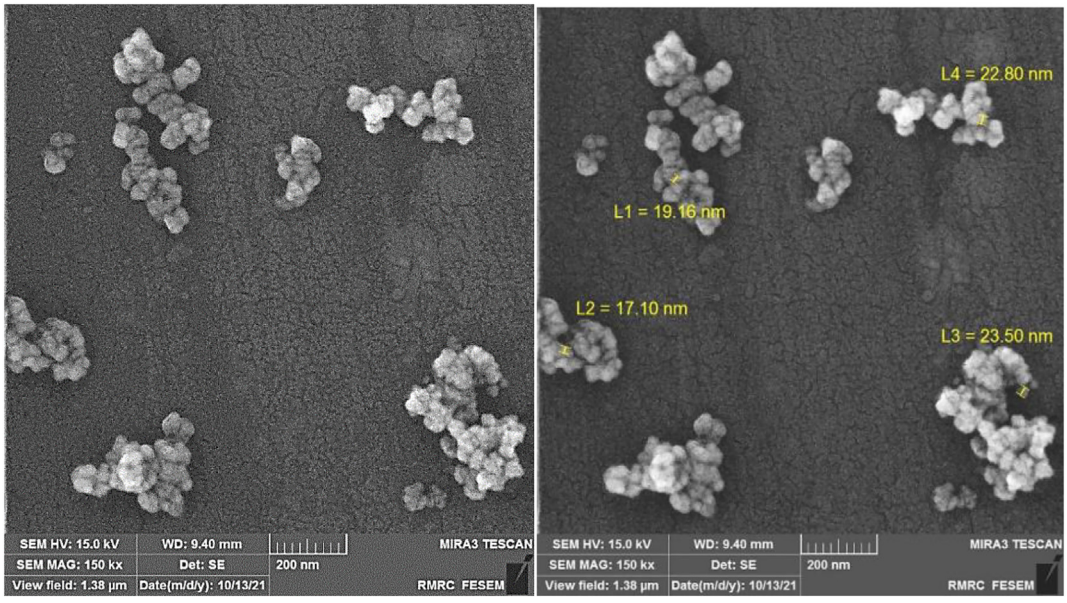

Fig. 6 FESEM image showed the Amorphous Mesoporous Silica Nanoparticles.

ical properties, reduces the fluid loss of the mud, and causes a slight change in the pH of the mud. So, to investigate the effect of AMSN on Shale recovery, the base mud and the mud containing 0.1 w/w AMSN are compared (see Table 3).

According to the American Petroleum Institute standard API RP 13I method, the Shale recovery test was performed (API, 2009). This experiment simulates the conditions of drilling cuttings exposed to drilling fluid during transfer to the surface in the annular space of the wellbore. The drilled Shale sample was milled and sieved with mesh five (4 mm) and ten (2 mm). The fine Shale particles that passed through mesh five but remained on mesh ten were used for the experiment. 20 g of the granulated Shale sample was added to a container, including 350 mL of each fluid sample. The Shale and drilling fluid sample cell were placed in a rolling oven for 8 hr at 121.1 °C. After the test period, the cell was cooled to room temperature. A mixture of 15 lb per barrel of potassium chloride and saturated brine was prepared as the washing solution. Afterward, the Shale particles were poured into a 35-mesh sieve and were washed with a washing solution made (see Fig. 4). Then Shale particles were dried in an oven at

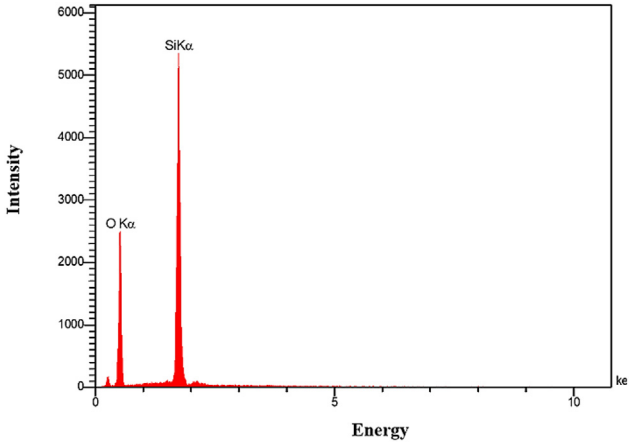

Fig. 7 EDX results test for AMSN.

121.1 °C, and the Shale sample was weighed. The Shale recovery percentage was determined by Eq. (7), (Rana et al., 2020; Saleh et al., 2022; Al-Arfaj et al., 2018).

Table 5 Elemental detected from EDX analysis.

Components	Si	O	K	Ca	Mg	Na
Weight%	36.58	63.42	0.00	0.00	0.00	0.00

Table 6 XRF test results for Nano-Silica synthesized.

Composition	SiO_2	P_2O_5	Fe_2O_3	K_2O	CaO	Cl	Na_2O	Al_2O_3	TiO_2	L.O. I
Weight%	98.99	N. D	0.01	N. D	N. D	N. D	N. D	0.01	N. D	0.99

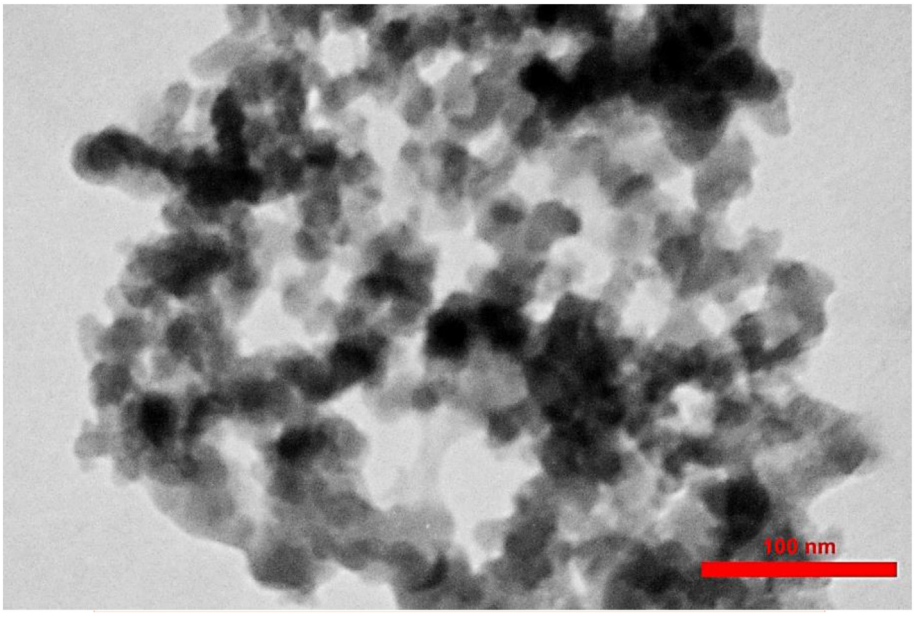

Fig. 8 TEM image showed the Mesoporous Amorphous Silica Nanoparticles (AMSN).

$$Shale\ Recovery = \frac{weight\ of\ Recovered\ shale\ sample}{weight\ of\ Initial\ shale\ sample} * 100 \quad (7)$$

2.6. Thermal stability test

In this step, the performance of the base drilling mud and the mud containing 0.1% w/w of AMSN in the presence of Shale at 148.8 °C was investigated (see Fig. 5). mud properties were measured after 8 hr of heating and rolling at 148.8 °C. Table 4 reports the results of these tests.

3. Result and discussion

3.1. AMSN analysis

- *FESEM test*

Nanoparticles (NPs) must have conductive surfaces in order to be photographed microscopically. As a result of the non-conductivity of AMSN's surface, the surface of AMSN is covered with gold atoms (Zarei et al., 2021). Field Emission Scanning Electron Microscopy (FESEM) model MIRA3-TESCAN-XMU was used to photograph the surface of the synthesized AMSN (Feng et al., 2023). The images were taken at 200 nm and presented in Fig. 6.

- *EDX test*

By performing elemental analysis on the synthesized materials, each element's chemical composition and weight percentage in the sample can be determined. By executing Energy Dispersive X-ray Spectroscopy (EDX) analysis on the synthesized Nano Silica powder, the values of each element were determined and reported in Fig. 7 and Table 5.

- *XRF test*

X-ray fluorescence (XRF) spectroscopy based on the type and intensity of fluorescence waves emitted from the synthesized samples could be determined the chemical composition and values of each component. XRF test has been conducted on the synthesized sampling using ARL 8410 apparatus, and its results are presented in Table 6.

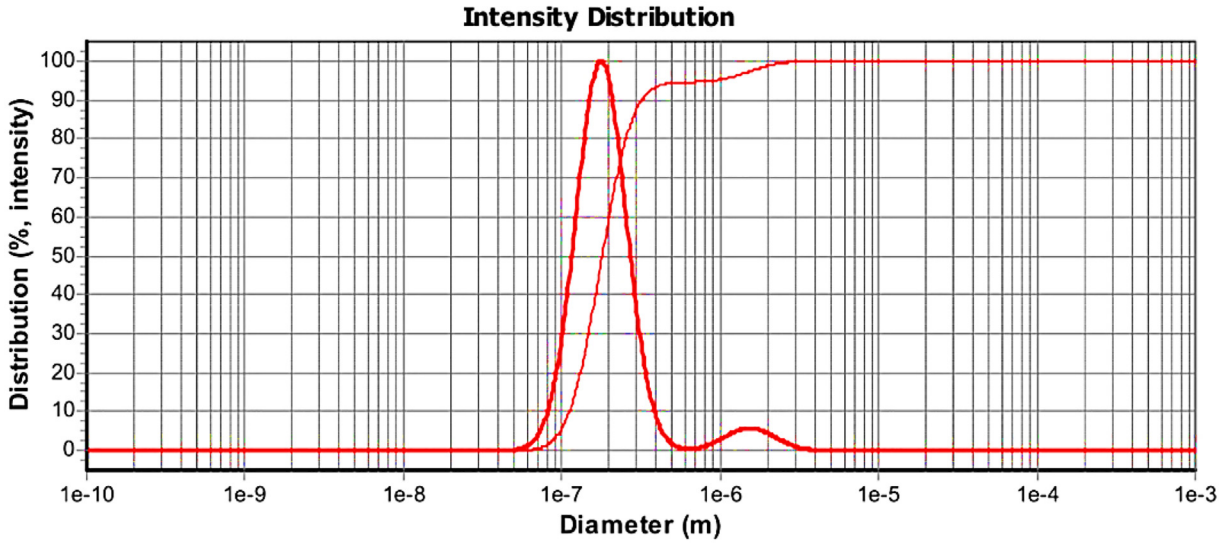

Fig. 9 DLS test results.

Table 7 BET test results for AMSN synthesized.

BET range limit (p/p_0 = 0.2762)	9-point number	Unit
$a_{s,\ BET}$	226.13	[$m^2\ g^{-1}$]
Total pore volume (p/p_0 = 0.990)	1.0539	[$cm^3\ g^{-1}$]
Mean pore diameter	18.642	[nm]

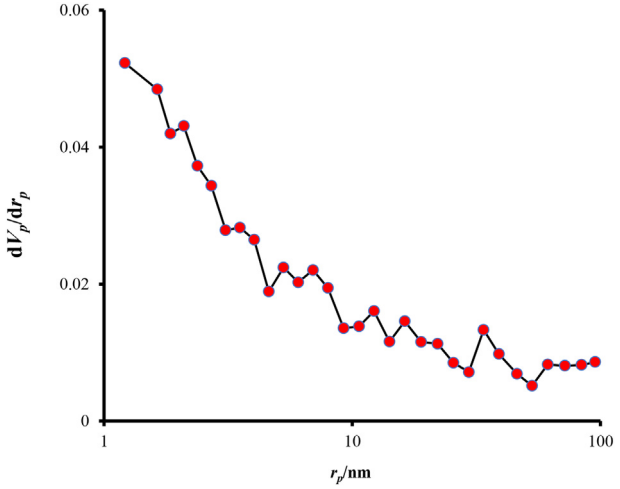

Fig. 10 BJH test results.

- *TEM test*

Transmission electron microscopy (TEM) model Zeiss LEO-906 Germany, operating at 80KeV, was used to show the mesopore created during the synthesis of Nanoparticles. The image taken is presented in Fig. 8.

- *Nanoparticle size analyzer*

To determine the particle size of synthesized AMSN, used Dynamic Light Scattering (DLS) apparatus model Scatteroscope I, Qudix, Korea (Mousavipour et al., 2021). The results of this analysis are shown in Fig. 9.

- *Surface area and pore size analyzers*

The BET (Brunauer, Emmet, and Teller) and BJH (Barrett, Joyner, and Halenda) theories are the famous models used to determine the Specific Surface Area (SSA), porosity volume, mean pore diameter, and procedure for calculating pore size distributions respectively. To measure these parameters for synthesized AMSN, the apparatus model TriStar II Plus, USA, was used. The results of this analysis are shown in Table 7 and Fig. 10.

- *XRD test*

X-RAY Diffraction spectrometer (XRD) analysis was used to determine the amorphous or crystalline phase of the synthesized AMSN by apparatus model (X'Pert PRO-MPD PANalytical, Netherlands). The X-ray diffraction patterns are shown in Fig. 11.

3.2. AMSN characterizations

So that had better know the synthesized AMSN, several analyzes have been performed to show the properties. Evaluating the size of AMSN by FESEM showed that particles have Nano-size (Fig. 6). Furthermore, DLS analysis confirms that the synthesized AMSN has Nano-size spectrums. DLS trial reported that the size of AMSN ranged from 50 nm to 4.5 um, with the average size D50 of 180 nm and D90 of 300 nm (Fig. 10).

Solid pores can be classified into three categories based on their pore size. Solids with a pore size below 2 Nanometers or in the range of 2 nm contain micro-pores, pore sizes between 2 and 50 nm indicate mesopores, and pore sizes larger than 50 nm are called macropores (Davis, 2002). Hence, the results of BET analysis have revealed the presence of Nanometer pores with an average pore diameter of 18 nm (Table 7), which indicates AMSN classified at mesoporous materials. As shown

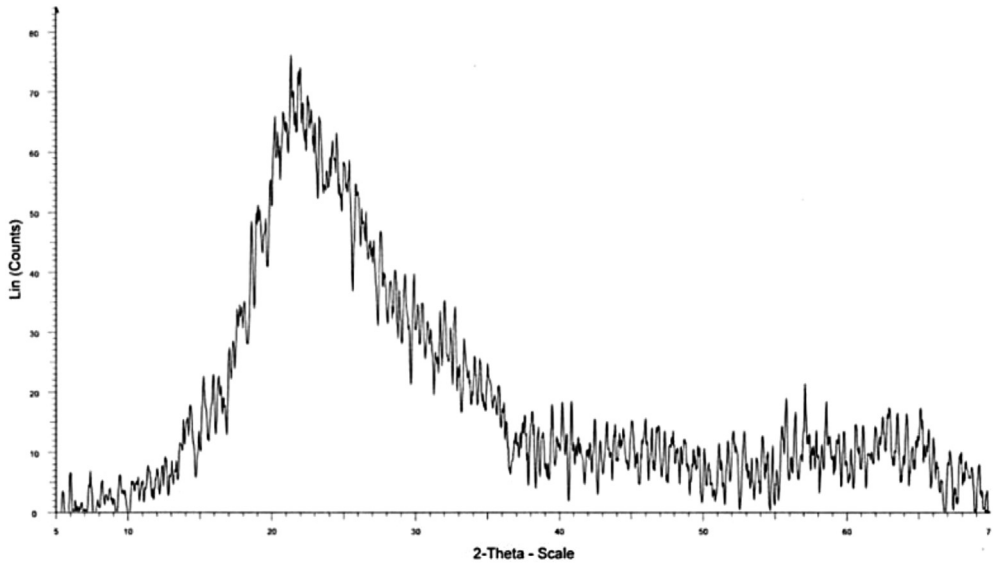

Fig. 11 XRD test results.

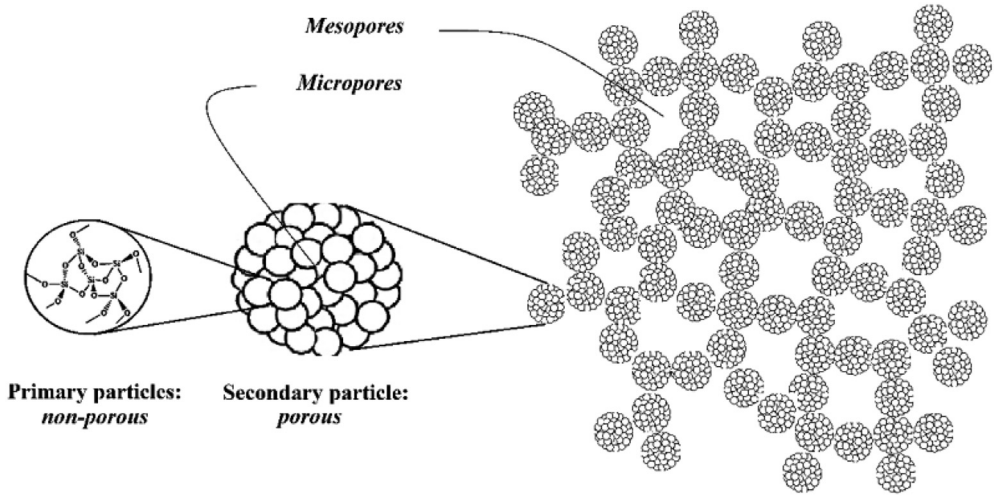

Fig. 12 Stepwise of forming Amorphous Mesoporous Silica Nanostructure.

Table 8 The Shale sample mineralogy.

No.	Mineral	Content, wt%
1	**Cristobalite**	49.6
2	**Montmorillonite**	21.1
3	**Quartz**	13.2
4	**Kaolinite**	8.7
5	**Calcite**	7.4

by the TEM image of the synthesized Nanoparticles in Fig. 8, which form the pearl necklace network, secondary particles in mesoporous materials are composed of compacted Silica primary particles. This is confirmed by the schematic shown in Fig. 12, for mesoporous materials (Zhang et al., 2004).

The results of the BJH isotherm reported in Fig. 9, represented the pore size distribution pattern. As shown in Fig. 9, pores in the range of 2 nm have the highest distribution, and with an increasing radius, the distribution of pores decreases. This pore size can belong to the channels between the primary particles. Pores with dimensions of 2 to 50 nm are the space

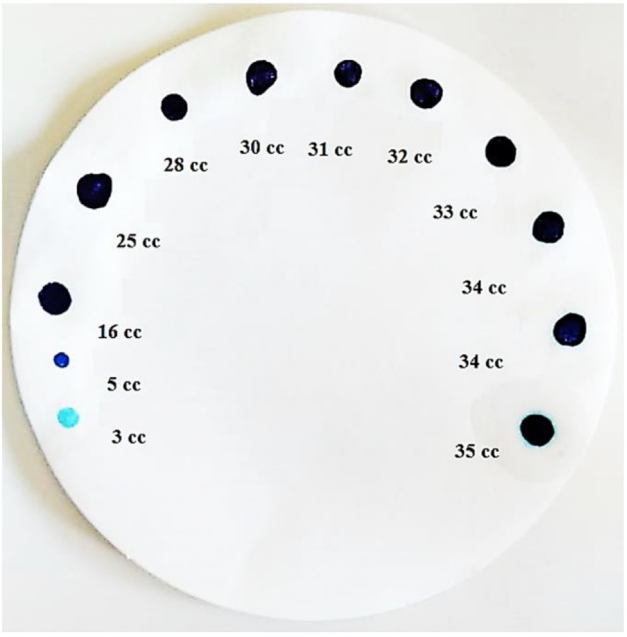

Fig. 13 The Methylene blue titration endpoint spot tests.

between the secondary particles that are classified in the range of mesopores (See Fig. 12). The surface area of AMSN was obtained by BET analysis at 226.13 (m^2 g^{-1}), (Table 7).

The elemental analysis of the EDX test results on the synthesized powder sample shows four peaks on the graph (see Fig. 7). The first peak has small values and is related to the gold atom used to cover the powder sample for microscopic photography. The second and third peaks, with weight percent of 36.58 and 63.42, are related to the two elements silicon and oxygen, respectively. Finally, the last peak is related to the elements whose values were so small that the device could not detect them. XRF analysis has been performed to determine the chemical composition. The type of chemical composition synthesized is silicon dioxide (SiO_2), and its purity percentage is 98.99% (Table 6).

Fig. 11 shows the results of the X-ray diffraction pattern of the synthesized AMSN. This pattern shows that only a wide peak is observed in the 23° (2θ) range, representing the Silica material. The large width of the peak, 15° to 30°, always confirms that the Silica phase is amorphous (Liu et al., 2007). Also, no other peaks are observed in this range, which confirms the high purity of the synthesized sample without creating an unwanted phase during the synthesis process (Tadjarodi et al., 2012), (Thuadaij and Nuntiya, 2008).

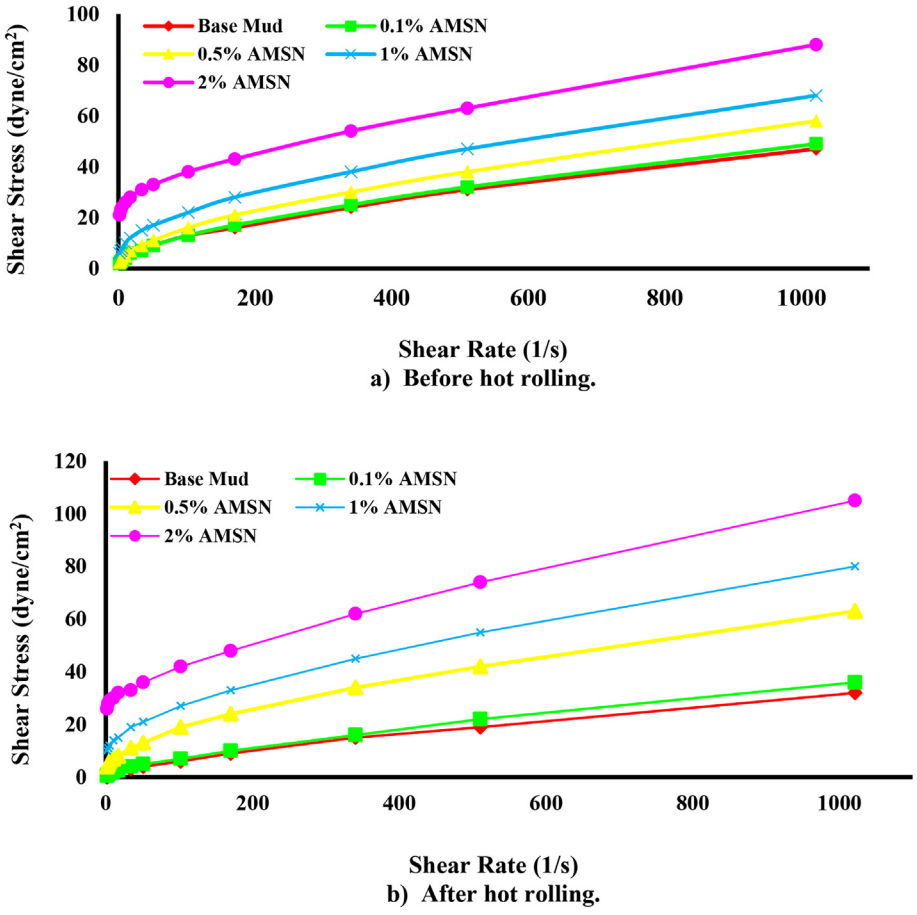

Fig. 14 Shear stress versus shear rate, up to down; a) before hot rolling. b) After hot rolling (121.1 ℃).

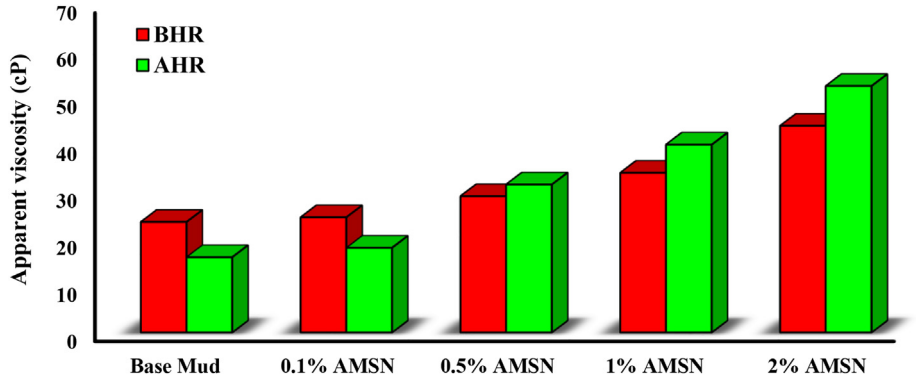

Fig. 15 Impact of synthesized AMSN on apparent viscosity.

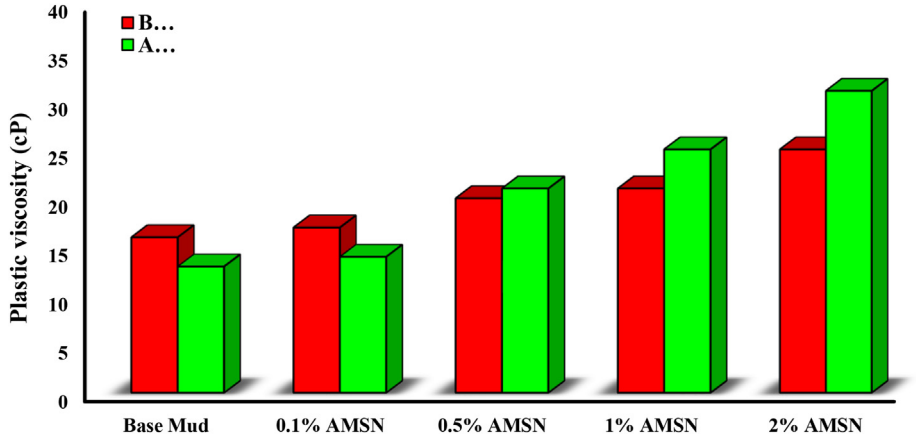

Fig. 16 Impact of synthesized AMSN on plastic viscosity.

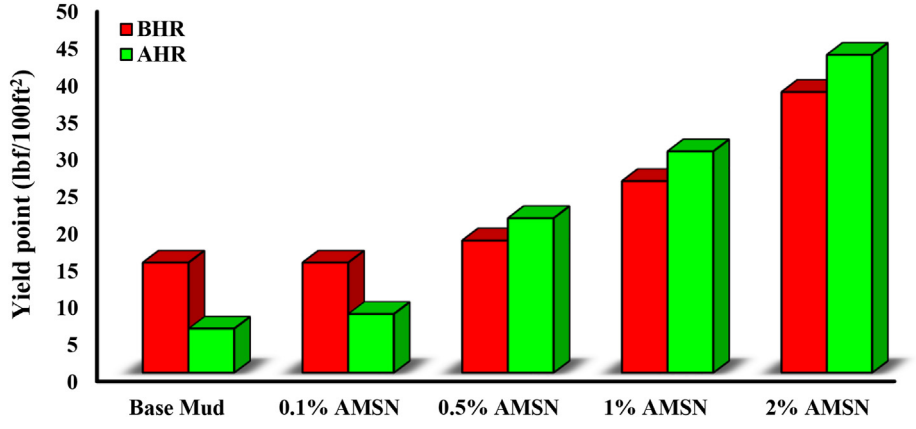

Fig. 17 Impact of synthesized AMSN on yield point.

3.3. Shale characterizations

X-ray diffraction analysis determined the mineral content of the Shale samples. The XRD test of the Shale was done using XRD equipment (GNR Explorer, Italy). The Cu-Kα (λ = 0. 154 nm) at the voltage of 40 kV and operating current of 30 mA. The samples were scanned at a scan rate of 1/sec in the 2θ range of 5$\circ$ to 90$\circ$. Table 8 shows the mineralogical composition of the Shale samples (Msadok et al., 2020).

- *Methylene blue test (MBT)*

Methylene blue ($C_{16}H_{18}N_3SCl$) eliminates exchangeable cations from clay minerals, which are absorbed by clay particles simultaneously. The absorption of methylene blue on the

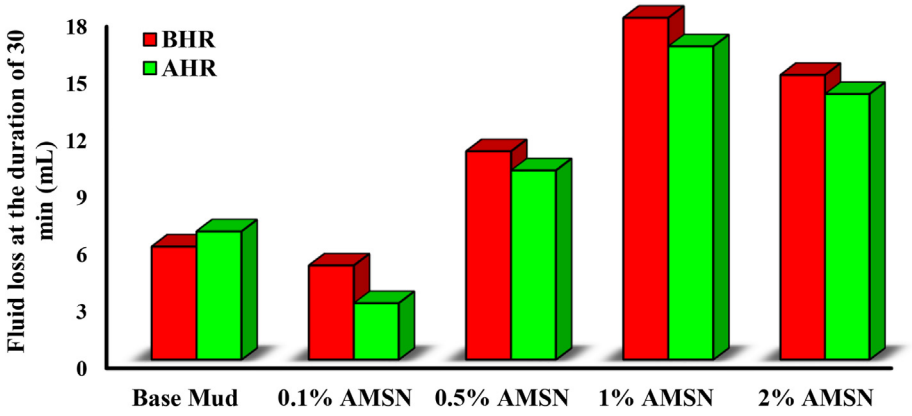

Fig. 18 Impact of synthesized AMSN on fluid loss.

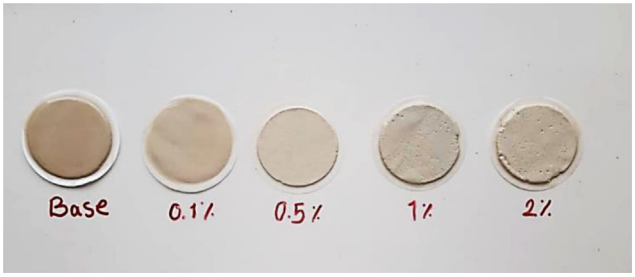

Fig. 19 Picture of mud cakes after hot rolling.

Shale surface can be used to calculate Shale's cation exchange capacity (CEC). The MBT procedure is as follows:

1. Add 50 mL of tetrasodium pyrophosphate solution (2%) to the Erlenmeyer flask containing 0.5 gr Shale.
2. Stir thoroughly and boil gently for 10 min on low heat. Boiling to a dry state is not recommended.
3. Allow cooling to ambient temperature before adding water to make a volume of roughly 50 mL.
4. With an accurate burette, add 1 mL increments of Methylene blue solution to the flask while stirring on the magnetic stirrer. Since the endpoint should only be achieved when 25 mL or more has been added, somewhat greater increments (10 mL to 15 mL) can be used at the start of the titration. Stir the flask's contents for 30 s after each addition, then extract one drop of the suspension and place it on the filter paper. The titration has achieved its initial endpoint when the dye shows as a faint turquoise ring or halo surrounding the stained solids. It is advised that increments of no more than 1 mL be utilized for more accuracy.
5. When the first endpoint is reached, stir the flask for another 2 min before dropping another drop onto the test paper. The endpoint has been reached if the faint turquoise ring or halo appears again.

Eq. (8) is used to compute the Methylene blue capacity of the Shale $C_{MBT-Shale}$ expressed in milliequivalents per hundred grams (meq/100gr).

Table 9 The cation exchange capacity of some clay minerals.

Clay Mineral	CEC (mEq/100 g)
Kaolinite	3–15
Halloysite	5–50
Ilite	10–40
Chlorite	10–40
Montmorillonite	60–150
Vermiculite	100–150

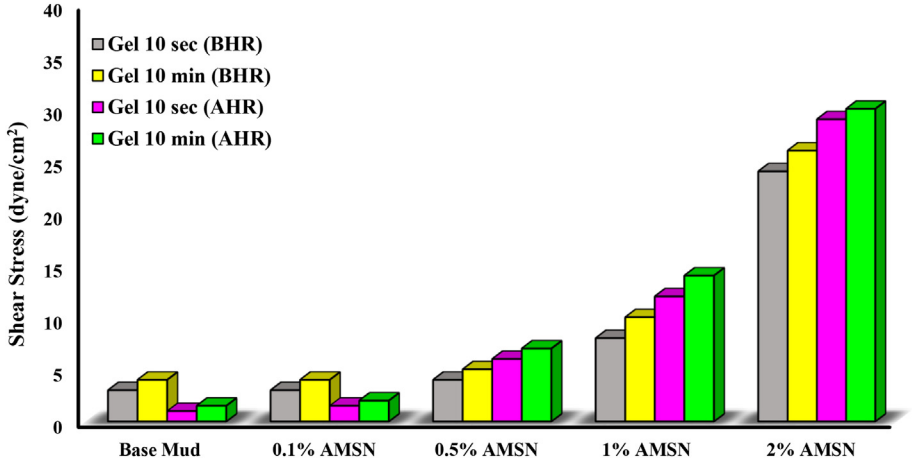

Fig. 20 Impact of synthesized AMSN on gel strength.

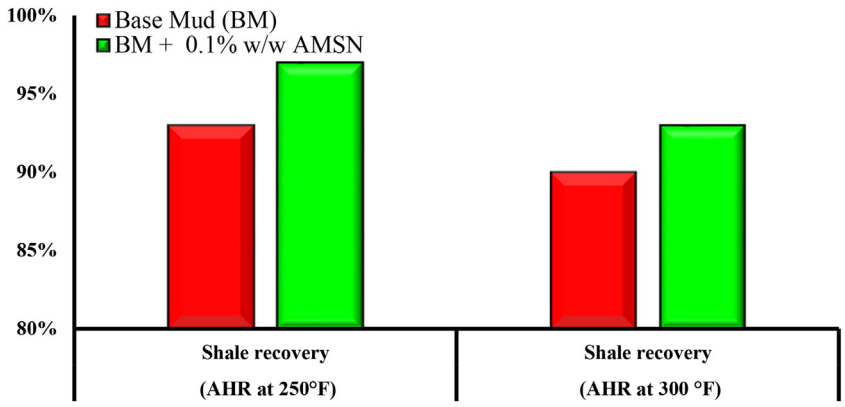

Fig. 21 Impact of synthesized AMSN on Shale recovery at different temperatures.

$$C_{MBT-Shale} = \frac{V}{m_{Shale}} \quad (8)$$

V denotes the volume of Methylene blue solution used in the titration in mL, and m denotes the mass of the Shale sample in grams. Fig. 13 depicts the spot tests for the Methylene blue titration endpoint and the turquoise ring around the drops at the end of the test. According to the Methylene blue test, the cation exchange capacity of the Shale is 75 meq/kg (API RP 13B-1, 2017), (Rezaei and Shadizadeh, 2021).

3.4. Drilling fluid characterization

- *Shear Stress*

Shear stresses $(dyne/cm^2)$ of the mud samples were measured by using the viscometer at 1, 2, 3, 6, 10, 20, 30, 60, 100, 200, 300, and 600 rpm before and after heating. According to the bob and rotor of the viscometer, which is R1B1, the shear rate constant of the viscometer is equal to 1.7023 $(sec^{-1}\, per\, rpm)$: therefore, the shear rates according to mentioned rpms are 1.7, 3.4, 5.11, 10.21, 17.02, 34.05, 51.07, 102.14, 170.23, 340.46, 510.69 and 1021.38 (sec^{-1}) respectively.

The results show that AMSN increases the shear profile of mud samples. With increasing the concentration of AMSN, the shear stress also increases. Fig. 14(a) shows the shear profile of the mud samples at 43.3 ℃ before heating. Fig. 14(b) shows that the shear profile of the mud samples was read at 60 ℃ after 4 hr of rolling and heating at 121.1 °C. It can be seen that the shear profile of the base mud has decreased due to heating and rolling, but with increasing the concentration of AMSN, the shear profile before and after heating has increased.

- *Apparent viscosity*

The apparent viscosity in the Bingham plastic model is one-half of a dial reading at 600 rpm. As shown in Fig. 15, adding AMSN to the base mud increases the apparent viscosity before and after hot rolling. The increase in apparent viscosity occurs due to the chemical activity of the AMSN. The functional groups in AMSN cause proper bonding of polymers through colloidal forces, which increases the apparent viscosity of drilling muds (Zarei and Nasiri, 2021). The highest apparent viscosity occurs at a concentration of 2% w/w AMSN.

- *Plastic viscosity*

When a drilling fluid has a high PV, it loses its pumpability, and high values of forces are needed to move the drilling fluid. On the other hand, when the drilling fluid has a low PV, it will not be able to transfer drilled cuttings and solid particles in the mud from the bottom of the well to the surface (Esfandyari Bayat et al., 2021). Polymer additives in the drilling fluid are degraded due to increasing temperature during the drilling operation, which will reduce the plastic viscosity

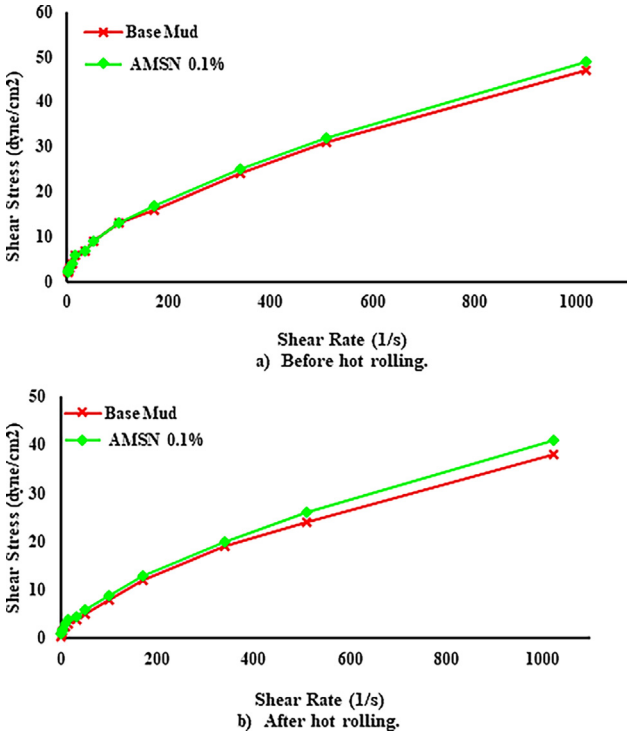

Fig. 22 Impact of synthesized AMSN on Shear stress up to down; a) before hot rolling. b) After hot rolling (121.1 ℃).

properties of the drilling fluid (Perumalsamy et al., 2021). Therefore, drilling fluid needs an additive to maintain or enhance this property.

As shown in Fig. 16, PV decreases when the base mud is placed in the simulated downhole condition. While at the same time, adding AMSN to the base mud before and after the hot rolling increases PV. The rise of the concentration of AMSN leads to an addition in plastic viscosity. Because with the addition of AMSN, the solid particles in the fluid will rise, consequently reducing the distance between the particles. As the distance between the particles reduces, more physical contact is raised, which leads to an elevation in the friction force. Increased friction increases the fluid resistance to motion, interpreted as risen plastic viscosity (zarei et al., 2018). The highest PV was obtained when the highest concentration of AMSN was applied (i.e., a concentration of 2% w/w).

- *Yield point*

The yield point of a fluid is due to electrochemical forces created by electrical charges on the surface of reactive particles. The yield point directly affects the ability of the fluid to carry solid particles and drilled cuttings from inside the well to the surface (Esfandyari Bayat et al., 2021). The experimental results show that the yield point of the base mud is reduced by placing it in the simulated downhole conditions. Adding AMSN to the base mud increases the yield point before and after heating. The highest yield point is obtained when the highest concentration of AMSN was applied (i.e., a concentration of 2% w/w), (see Fig. 17). An excessive increase of the yield point also reduces the pump-ability of the drilling muds, so Nanoparticles should always be used at the optimal concentration in the fluid.

- *fluid loss*

Fig. 18 shows that placing the base mud at the simulated downhole temperature increases filtration. One of the main reasons for increasing the fluid loss of the base mud in heating and rolling is the breakage of the polymer chains related to thermal degradation. In some cases, adding AMSN to the base mud increases the filter loss and, in other cases, decreases the amount of filter loss. When Nanoparticles are utilized in optimal concentration, the presence of Nanoparticles in drilling mud counteracts the effect of hot rolling on LPLT fluid loss, or in other words, it thermally stabilizes the LPLT fluid loss of drilling mud. These results demonstrate the ability of particles of nano to plug the pores of filter cake generated during

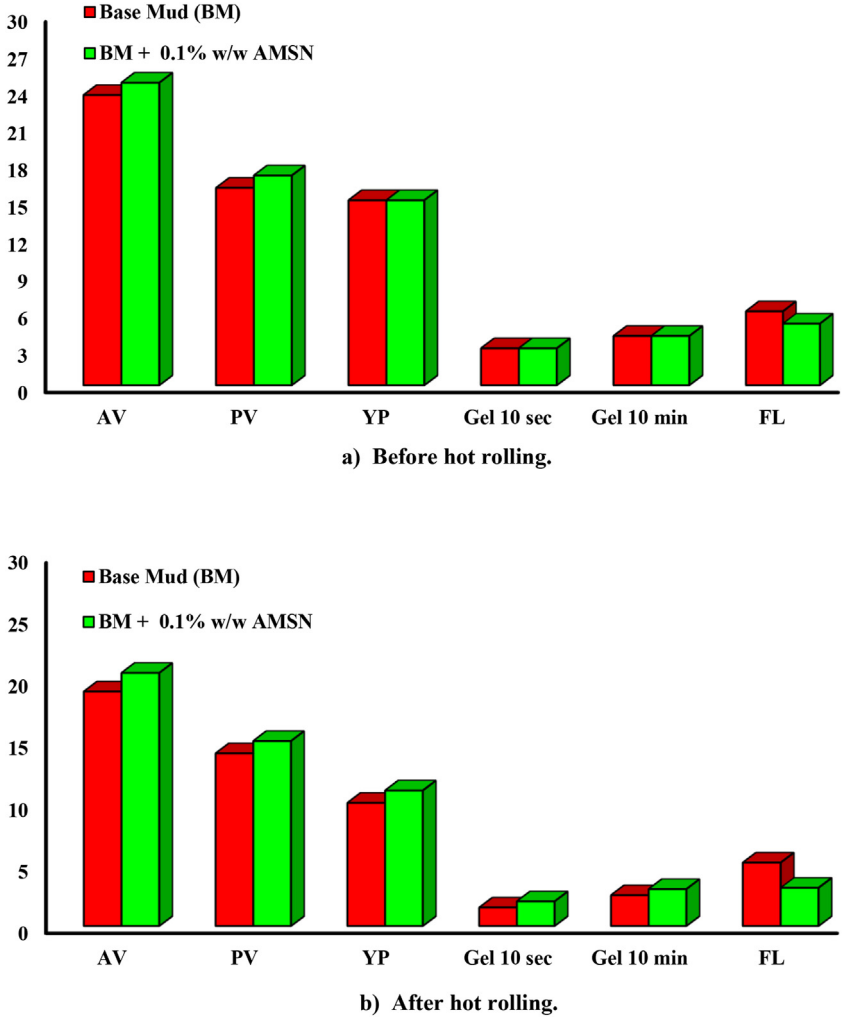

Fig. 23 Impact of synthesized AMSN on rheological properties, up to down; a) before hot rolling. b) After hot rolling (121.1 ℃).

filtering, resulting in lower permeability and LPLT fluid loss (Beg et al., 2019, Srivastava et al., 2021).

At high concentrations of AMSN, accumulation and aggregation of particles occur, causing some pores in the mud cake of the samples before and after the heating and rolling process. Pores in these mud cakes increase the permeability of the mud cake so that there is an increased amount of filtration. Fig. 19 shows the image of mud cakes after hot rolling for 4 hr at 121.1 ℃. When AMSN are used in optimal concentrations, creating a homogeneous cake with the lowest permeability, reduces fluid loss before and after the hot rolling. The mud cake thickness for base mud and Silica Nanoparticle concentrations of 0.1, 0.5, 1%, and 2% by weight is 1.5, 1, 1.7, 2.2, and 2.5 mm, respectively.

Fig. 18 shows that the mud sample containing 0.1% w/w of AMSN has the lowest filter loss, so the concentration of 0.1% w/w of AMSN is optimal. As shown in Fig. 19, the mud sample containing 0.1% w/w of AMSN has the lowest thickness compared to other mud cakes and without pores. Pores have developed on the mud cakes at concentrations of 0.5, 1, and 2% w/w of AMSN, proving that these concentrations are not optimal. Because in these concentrations, aggregation of the particles has happened.

- *pH*

According to the experimental results, adding AMSN to the drilling mud samples reduces the pH of the drilling mud. In water-based muds, AMSN reacts with the hydroxyl anions, decreasing the pH. In Table 6, the lowest pH is obtained at a 2% w/w AMSN concentration. A series of reactions between AMSN and hydroxyl anions in Eq (9) and (10) could occur (Piroozian et al., 2012; Kang et al., 2016).

$$SiO_2 + 2NaOH \rightarrow Na_2OSiO_2 + H_2O \quad (9)$$

$$SiO_2 + NaOH + H_2O \rightarrow NaH_3SiO_4 \quad (10)$$

- *Gel Strength*

Gel strength demonstrates the drilling fluid's ability to suspend solid particles when the drilling fluid rotation is stopped and the fluid column is in a static state (Al-Yasiri et al., 2019). The gel strength of the drilling fluid is due to the electrochemical forces in the fluid system in static conditions (Shakib et al., 2016). Gel strength measurement is made on the viscometer using the 3-rpm reading, which will be recorded after stirring the drilling fluid at 600 rpm to break the Gel. The first reading, known as initial gel strength, is noted after the mud is in a static condition for 10 s (Kania et al., 2021; Du et al., 2020). The second reading, called final gel strength, will be measured after 10 min. As shown in Fig. 20, adding AMSN to the drilling fluid increases the gel strength of the fluid before and after the hot rolling test. It can be seen the gel strength increases with increasing AMSN concentration, and the highest gel strength is obtained when the highest concentration of AMSN was applied (i.e., a concentration of 2% w/w).

- *Shale Recovery*

Table 9 shows the cation exchange capacity values for different clay minerals (Schwanke and Pergher, 2013, Bain and Smith, 1994). According to the MBT test, the CEC of the Shale is equal to 70 (See Fig. 13). As a result, Montmorillonite is the Shale used in the Shale recovery tests in this paper. Moreover, the XRD analysis of the Shale indicates that it contains 21.1% of Montmorillonite. This Caly which belongs to the Smectites class, has the second-highest cation exchange capacity. Because of their high negative charge and small particle size, Smectite clays have the most remarkable ability to swell and disperse (Rowell, 2014).

The experimental results showed that a concentration of 0.1% w/w of AMSN improved all the base fluid properties and had no adverse effect on the base fluid, so it was introduced as the optimal concentration. A Shale recovery test was performed for base fluid and fluid containing 0.1% w/w of AMSN. The results of the Shale recovery test showed that AMSN increased Shale recovery (see Fig. 21).

AMSN plugs the pores on Shale particles and prevents water from diffusing into the Shale (Ahmad et al., 2021; Hoxha et al., 2019; zarei et al., 2018). In addition, the functional groups on the AMSN interact with the surface charges on Shale and inhibit the hydration of Shale particles (Saleh and Ibrahim, 2019). Polymers in drilling fluid also play a vital role in reducing Shale hydration, swelling, and dispersion (Azad et al., 2018a). The polymers create a hydrophobic protective layer around the Shale and encapsulate it to prevent direct contact of water with the Shale particles. In this manner, hydrophilic parts of the polymer chains adhere to the Shale's hydrophilic parts, and the polymers' hydrophobic parts pre-

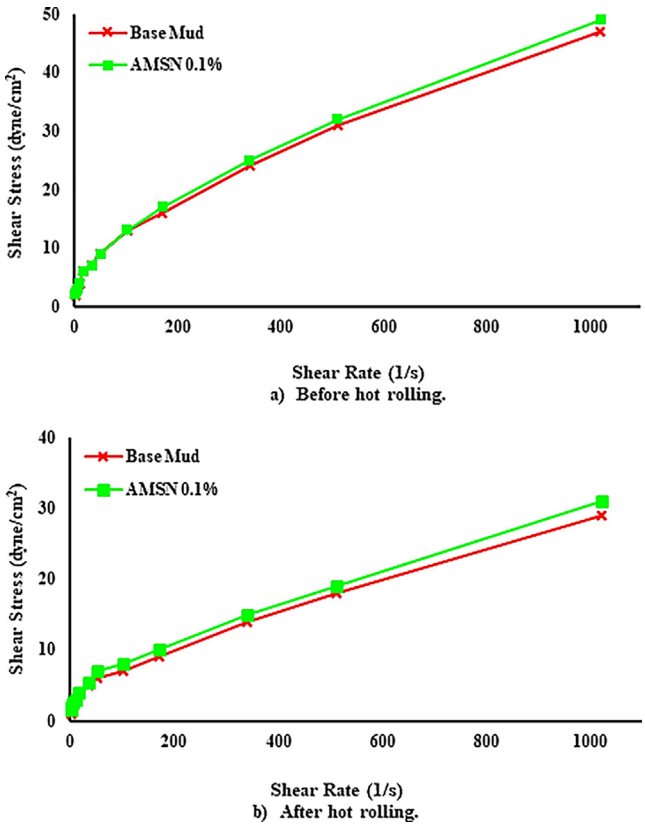

Fig. 24 Impact of synthesized AMSN on Shear stress, up to down; a) before hot rolling. b) After hot rolling (148.8 ℃).

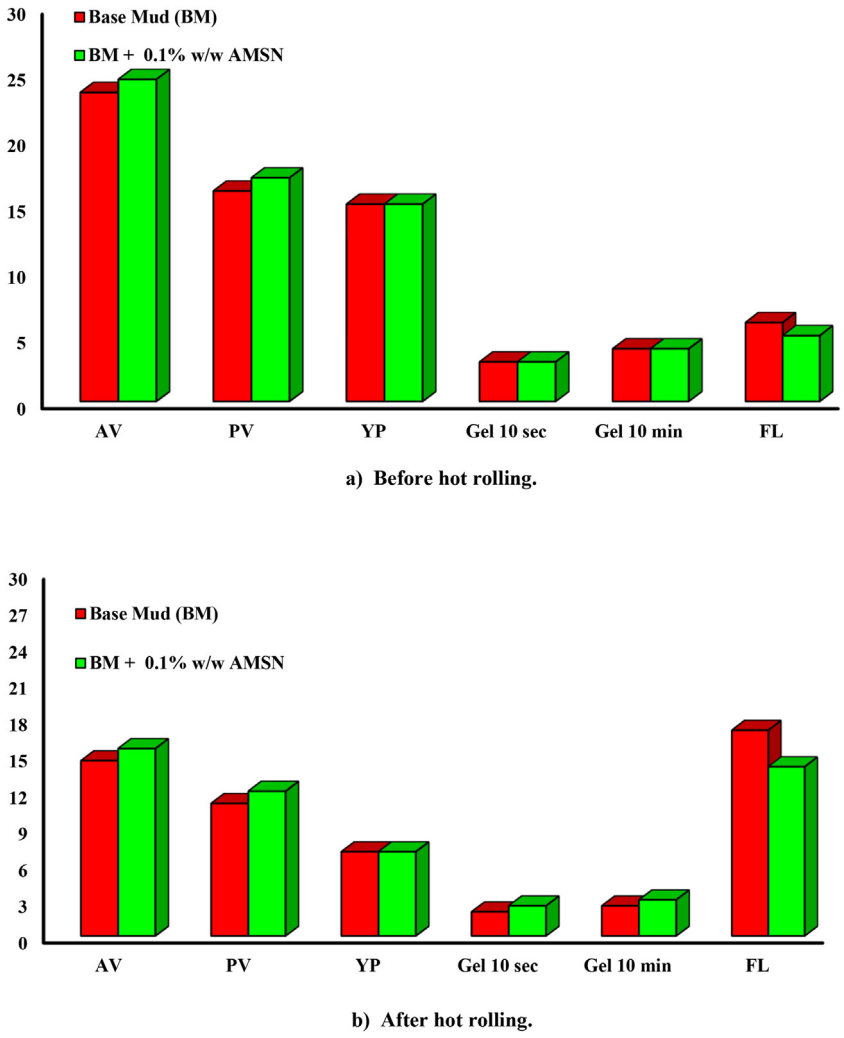

Fig. 25 Impact of AMSN on rheological properties, up to down; a) before hot rolling. b) After hot rolling (148.8 ℃).

Fig. 26 Mud cake dissolves rapidly in 25% hydrochloric acid.

vent water from approaching the Shale (Azad et al., 2018b). Fig. 22 shows that adding AMSN to this fluid increases the shear stress. The presence of Shale also improves the rheological properties and filtration of the base fluid. As shown in Fig. 23, the small amount of Shale dispersed in the drilling fluid improves the rheological properties and reduces the filtration of the drilling fluids.

- *Thermal Stability*

In order to evaluate the thermal stability of the designed drilling fluid in simulated downhole conditions in the presence of drilling cuttings, a new experiment was designed. The base fluid and the drilling fluid containing 0.1% w/w of AMSN with 20 g of Shale were heated and rolled for 8 hr at 148.8 ℃. Then their properties were measured at 60 ℃. The results show that AMSN enhanced rheological properties, decreased fluid loss, and increased Shale recovery.

Fig. 24 shows that AMSN increased shear stress compared to base fluid before and after hot rolling. Fig. 25 shows that AMSN enhanced the AV, PV, and FL before and after hot

rolling but did not affect the yield point. It can be seen that AMSN improved the GS after hot rolling in the presence of Shale particles.

- *Formation Damage*

A new experiment was developed to determine the risk of Formation damage caused by the designed drilling fluid under simulated downhole conditions. In this experiment, the drilling fluid was heated and rolled at 121.1 °C for eight hr with 0.1% w/w AMSN and 20 g of Shale. Following that, an LPLT filter press was used to prepare the mud cake. An oven at 105 °C was used to dry the mud cake. The mud cake was then treated with hydrochloric acid 25 %. All of the mud cake's contents dissolve rapidly in the acid (See Fig. 26), and when the solution passes through the filter paper, nothing remains, and it does so fast. Since Silica Nanoparticles are nanometric in size, they do not cause Formation damage despite not dissolving in hydrochloric acid. Because when other additives are dissolved, Nanoparticles are released, and with the production fluid flow, Nanoparticles with too fine also flow.

4. Conclusion

This paper studies drilling fluid and Shale stabilizing by using Nanotechnology. This research synthesized Amorphous Mesoporous Silica Nanoparticles (AMSN) with heightened purity and suitable surface area using the Sol–gel method. Utilizing AMSN, an environmentally friendly water-based drilling fluid with increased rheological properties and Shale recovery, has been designed. The results showed that applying AMSN in the muds prepared has advanced thermal stability. The main results are as follows:

(1) By assessing the AMSN, it was seen that the phase of AMSN is amorphous, and its purity, special surface area and total pore volume are 98.98%, 226.13 (m^2 g^{-1}), and 1.0539 (m^3 g^{-1}), respectively.
(2) Designed drilling mud is environmentally friendly and does not contain chemical substances Shale inhibitors.
(3) Evaluation of the rheological properties of the base fluid and fluids containing AMSN before and after heating showed that adding AMSN improves the rheological properties before and after heating.
(4) Between concentrations of 0.1, 0.5, 1, and 2% w/w of AMSN used in this study, a concentration of 0.1% improves all the drilling fluid properties. Concentrations of 0.5, 1, and 2% w/w increase FL and mud cake thickness.
(5) The results show that adding AMSN in the optimal concentration to the drilling fluid also increases the thermal stability and Shale recovery of the base fluid.
(6) Due to the use of calcium carbonate additive and other soluble materials in hydrochloric acid, this mud does not cause any damage to the production layers. Therefore, the designed drilling fluid in this study can be used for drilling reservoirs with high pressure and temperature.

CRediT authorship contribution statement

Vahid Zarei: Conceptualization, Methodology, Investigation, Visualization, Project administration, Software, Writing – original draft. **Hossein Yavari:** Conceptualization, Data curation, Formal analysis, Methodology, Resources, Validation. **Alireza Nasiri:** Supervision, Validation. **Mojtaba Mirzaasadi:** Investigation, Formal analysis, Funding acquisition. **Afshin Davarpanah:** Writing – review & editing.

References

Abbas, A.K., Alsaba, M.T., Al Dushaishi, M.F., 2021. Improving hole cleaning in horizontal wells by using nanocomposite water-based mud. J. Pet. Sci. Eng. 203,. https://doi.org/10.1016/j.petrol.2021.108619 108619.

Addagalla, A., Maley, I., Moroni, L., Khafagy, M., 2018. Nano-Technology Based Bridging System Helps Drilling Success in Highly Depleted Mature Fields, in: Abu Dhabi International Petroleum Exhibition & Conference. SPE. 10.2118/193153-MS.

Ahmad, H.M., Iqbal, T., Al Harthi, A., Kamal, M.S., 2021. Synergistic effect of polymer and nanoparticles on shale hydration and swelling performance of drilling fluids. J. Pet. Sci. Eng. 205,. https://doi.org/10.1016/j.petrol.2021.108763 108763.

Al-Arfaj, M.K., Amanullah, M., Mohammed, A.O., 2018. An enhanced experimental method to assess the shale inhibition durability of inhibitive water-based drilling fluids. Proc. SPE/IADC Middle East Drill. Technol. Conf. Exhib. 2018-Janua. 10.2118/189380-ms.

Al-Yasiri, M., Awad, A., Pervaiz, S., Wen, D., 2019. Influence of silica nanoparticles on the functionality of water-based drilling fluids. J. Pet. Sci. Eng. 179, 504–512. https://doi.org/10.1016/j.petrol.2019.04.081.

Annamalai, M., Dhinesh, B., Nanthagopal, K., SivaramaKrishnan, P., Lalvani, I.J., Parthasarathy, M., Annamalai, K., 2016. An assessment on performance, combustion and emission behavior of a diesel engine powered by ceria nanoparticle blended emulsified biofuel. Energy Convers. Manage. 123, 372–380. https://doi.org/10.1016/j.enconman.2016.06.062.

API RP 13B-1, 2009. Recommended practice for field testing water-based drilling fluids, in: API Recommentation 13B-1, ISO 10414: 2001. p. 121.

API RP 13B-1, 2017. Recommend Practice for Field Testing Water-Based Drilling Fluids - 13B-1. API Publ. Serv. 2008, 121.

API, 2009. Recommended practice for laboratory testing of drilling fluids-13I. Api Recomm. Pract. 8, 124.

Azad, M.S., Dalsania, Y., Trivedi, J.J., 2018a. Understanding the flow behaviour of copolymer and associative polymers in porous media using extensional viscosity characterization: Effect of hydrophobic association. Can. J. Chem. Eng. 96, 2498–2508. https://doi.org/10.1002/cjce.23169.

Azad, M.S., Dalsania, Y.K., Trivedi, J.J., 2018b. Capillary breakup extensional rheometry of associative and hydrolyzed polyacrylamide polymers for oil recovery applications. J. Appl. Polym. Sci. 135, 46253. https://doi.org/10.1002/app.46253.

Bain, D.C., Smith, B.F.L., 1994. Chemical analysis, in: Clay Mineralogy: Spectroscopic and Chemical Determinative Methods. Springer, pp. 300–332.

Barroso, A.L., Marcelino, C.P., Leal, A.B., Odum, D.M., Science, B., Lucena, C., Castro, F., Energy, G., Masculo, M., Castro, F., 2018. New generation nano technology drilling fluids application associated to geomechanic best practices: field trial record in Bahia-Brazil. Offshore Technology Conference. OnePetro, 1–12.

Bashir Abdullahi, M., Rajaei, K., Junin, R., Bayat, A.E., 2019. Appraising the impact of metal-oxide nanoparticles on rheological properties of HPAM in different electrolyte solutions for enhanced oil recovery. J. Pet. Sci. Eng. 172, 1057–1068. https://doi.org/10.1016/j.petrol.2018.09.013.

Bayat, A.E., Moghanloo, P.J., Piroozian, A., Rafati, R., 2018. Experimental investigation of rheological and filtration properties of water-based drilling fluids in presence of various nanoparticles. Colloids Surf. A Physicochem. Eng. Asp. 555, 256–263.

Bayat, A.E., Shams, R., 2019. Appraising the impacts of SiO2, ZnO and TiO_2 nanoparticles on rheological properties and shale

inhibition of water-based drilling muds. Colloids Surf. A Physicochem. Eng. Asp. 581,. https://doi.org/10.1016/j.colsurfa.2019.123792 123792.

Beg, M., Kesarwani, H., Sharma, S., Gandhi, R., Technology, P., 2019. Effect of CuO and ZnO nanoparticles on efficacy of poly 4-styrenesulfonic acid-co-maleic acid sodium salt for controlling HPHT filtration, in: Abu Dhabi International Petroleum Exhibition & Conference. OnePetro, pp. 1–11.

Bizhani, M., Rodriguez Corredor, F.E., Kuru, E., 2016. Quantitative evaluation of critical conditions required for effective hole cleaning in coiled-tubing drilling of horizontal wells. SPE Drill. Complet 31, 188–199.

Boyou, N.V., Ismail, I., Wan Sulaiman, W.R., Sharifi Haddad, A., Husein, N., Hui, H.T., Nadaraja, K., 2019. Experimental investigation of hole cleaning in directional drilling by using nano-enhanced water-based drilling fluids. J. Pet. Sci. Eng. 176, 220–231. https://doi.org/10.1016/j.petrol.2019.01.063.

Chaturvedi, K.R., Fogat, M., Sharma, T., 2021. Low Temperature rheological characterization of single-step silica nanofluids: an additive in refrigeration and gas hydrate drilling applications. J. Pet. Sci. Eng. 204,. https://doi.org/10.1016/j.petrol.2021.108742 108742.

Davis, M.E., 2002. Ordered porous materials for emerging applications. Nature 417, 813–821.

Dhinesh, B., Annamalai, M., 2018. A study on performance, combustion and emission behaviour of diesel engine powered by novel nano nerium oleander biofuel. J. Clean. Prod. 196, 74–83. https://doi.org/10.1016/j.jclepro.2018.06.002.

Du, M., Liu, P., Clode, P.L., Liu, J., Haq, B., Leong, Y., 2020. Impact of additives with opposing effects on the rheological properties of bentonite drilling mud: Flow, ageing, microstructure and preparation method. J. Pet. Sci. Eng. 192,. https://doi.org/10.1016/j.petrol.2020.107282 107282.

Elochukwu, H., Gholami, R., Dol, S.S., 2017. An approach to improve the cuttings carrying capacity of nanosilica based muds. J. Pet. Sci. Eng. 152, 309–316. https://doi.org/10.1016/j.petrol.2017.03.008.

Esfandyari Bayat, A., Harati, S., Kolivandi, H., 2021. Evaluation of rheological and filtration properties of a polymeric water-based drilling mud in presence of nano additives at various temperatures. Colloids Surf. A Physicochem. Eng. Asp. 627,. https://doi.org/10.1016/j.colsurfa.2021.127128 127128.

Feng, Y., Zarei, V., Mousavipour, N., 2023. Provision and assessment properties of nanoliposomes containing macroalgae extracts of Sargassum boveanume and Padina pavonica. LWT 175, 114194. https://doi.org/10.1016/j.lwt.2022.114194.

Folgar, C., Folz, D., Suchicital, C., Clark, D., 2007. Microstructural evolution in silica aerogel. J. Non Cryst. Solids 353, 1483–1490. https://doi.org/10.1016/j.jnoncrysol.2007.02.047.

Gbadamosi, A.O., Junin, R., Abdalla, Y., Agi, A., Oseh, J.O., 2019. Experimental investigation of the effects of silica nanoparticle on hole cleaning efficiency of water-based drilling mud. J. Pet. Sci. Eng. 172, 1226–1234. https://doi.org/10.1016/j.petrol.2018.09.097.

Harati, S., Esfandyari Bayat, A., Sarvestani, M.T., 2020. Assessing the effects of different gas types on stability of SiO_2 nanoparticle foam for enhanced oil recovery purpose. J. Mol. Liq. 313,. https://doi.org/10.1016/j.molliq.2020.113521 113521.

Hoxha, B.B., van Oort, E., Daigle, H., 2019. How do nanoparticles stabilize shale? SPE Drill. Complet. 43, 143–158. https://doi.org/10.2118/184574-PA.

Jafariesfad, N., Gong, Y., Geiker, M.R., Skalle, P., 2016. Nano-sized MgO with engineered expansive property for oil well cement systems. Soc. Pet. Eng. - SPE Bergen One Day Semin. https://doi.org/10.2118/180038-ms.

Jain, R., Mahto, V., Sharma, V.P., 2015. Evaluation of polyacrylamide-grafted-polyethylene glycol/silica nanocomposite as potential additive in water based drilling mud for reactive shale formation. J. Nat. Gas Sci. Eng. 26, 526–537. https://doi.org/10.1016/j.jngse.2015.06.051.

Jal, P.K., Sudarshan, M., Saha, A., Patel, S., Mishra, B.K., 2004. Synthesis and characterization of nanosilica prepared by precipitation method. Colloids Surf. A Physicochem. Eng. Asp. 240, 173–178. https://doi.org/10.1016/j.colsurfa.2004.03.021.

Kang, Y., She, J., Zhang, H., You, L., Yu, Y., Song, M., 2016. Alkali erosion of shale by high-pH fluid: Reaction kinetic behaviors and engineering responses. J. Nat. Gas Sci. Eng. 29, 201–210. https://doi.org/10.1016/j.jngse.2016.01.013.

Kania, D., Yunus, R., Omar, R., Rashid, S.A., Jan, B.M., Aulia, A., 2021. Lubricity performance of non-ionic surfactants in high-solid drilling fluids: a perspective from quantum chemical calculations and filtration properties. J. Pet. Sci. Eng. 207,. https://doi.org/10.1016/j.petrol.2021.109162 109162.

Karakosta, K., Mitropoulos, A.C., Kyzas, G.Z., 2021. A review in nanopolymers for drilling fluids applications. J. Mol. Struct. 1227,. https://doi.org/10.1016/j.molstruc.2020.129702 129702.

Katende, A., Boyou, N.V., Ismail, I., Chung, D.Z., Sagala, F., Hussein, N., Ismail, M.S., 2019. Improving the performance of oil based mud and water based mud in a high temperature hole using nanosilica nanoparticles. Colloids Surf. A Physicochem. Eng. Asp. 577, 645–673. https://doi.org/10.1016/j.colsurfa.2019.05.088.

Kök, M.V., Bal, B., 2019. Effects of silica nanoparticles on the performance of water-based drilling fluids. J. Pet. Sci. Eng. 180, 605–614. https://doi.org/10.1016/j.petrol.2019.05.069.

Liu, K., Feng, Q., Yang, Y., Zhang, G., Ou, L., Lu, Y., 2007. Preparation and characterization of amorphous silica nanowires from natural chrysotile. J. Non Cryst. Solids 353, 1534–1539. https://doi.org/10.1016/j.jnoncrysol.2007.01.033.

Ma, L., He, Y., Luo, P., Zhang, L., Yu, Y., 2018. Automatic dispersion, long-term stability of multi-walled carbon nanotubes in high concentration electrolytes. J. Nanoparticle Res. 20, 45. https://doi.org/10.1007/s11051-018-4148-z.

Mao, H., Qiu, Z., Shen, Z., Huang, W., 2015. Hydrophobic associated polymer based silica nanoparticles composite with core–shell structure as a filtrate reducer for drilling fluid at utra-high temperature. J. Pet. Sci. Eng. 129, 1–14. https://doi.org/10.1016/j.petrol.2015.03.003.

McElfresh, P., Wood, M., Ector, D., 2012. Stabilizing nano particle dispersions in high salinity, high temperature downhole environments. Soc. Pet. Eng. - SPE Int. Oilf. Nanotechnol. Conf. 2012, 40–45. https://doi.org/10.2118/154758-ms.

Mikhienkova, E.I., Lysakov, S.V., Neverov, A.L., Zhigarev, V.A., Minakov, A.V., Rudyak, V.Y., 2022. Experimental study on the influence of nanoparticles on oil-based drilling fluid properties. J. Pet. Sci. Eng. 208,. https://doi.org/10.1016/j.petrol.2021.109452 109452.

Mirzaasadi, M., Zarei, V., Elveny, M., Alizadeh, S.M., Alizadeh, V., Khan, A., 2021. Improving the rheological properties and thermal stability of water-based drilling fluid using biogenic silica nanoparticles. Energy Rep. 7, 6162–6171. https://doi.org/10.1016/j.egyr.2021.08.130.

Mousavipour, N., Babaei, S., Moghimipour, E., Moosavi-Nasab, M., Ceylan, Z., 2021. A novel perspective with characterized nanoliposomes: Limitation of lipid oxidation in fish oil. LWT - Food Sci. Technol. 152, 112387. https://doi.org/10.1016/j.lwt.2021.112387.

Msadok, I., Hamdi, N., Rodríguez, M.A., Ferrari, B., Srasra, E., 2020. Synthesis and characterization of Tunisian organoclay: application as viscosifier in oil drilling fluid. Chem. Eng. Res. Des. 153, 427–434.

Nanthagopal, K., Ashok, B., Garnepudi, R.S., Tarun, K.R., Dhinesh, B., 2019. Investigation on diethyl ether as an additive with Calophyllum Inophyllum biodiesel for CI engine application. Energy Convers. Manage. 179, 104–113. https://doi.org/10.1016/j.enconman.2018.10.064.

Novara, R., Rafati, R., Sharifi Haddad, A., 2021. Rheological and filtration property evaluations of the nano-based muds for drilling applications in low temperature environments. Colloids Surf. A

Physicochem. Eng. Asp. 622,. https://doi.org/10.1016/j.colsurfa.2021.126632 126632.
Oseh, J.O., Mohd Norddin, M.N.A., Ismail, I., Gbadamosi, A.O., Agi, A., Mohammed, H.N., 2019. A novel approach to enhance rheological and filtration properties of water–based mud using polypropylene–silica nanocomposite. J. Pet. Sci. Eng. 181,. https://doi.org/10.1016/j.petrol.2019.106264 106264.
Oseh, J.O., Norddin, M.N.A.M., Ismail, I., Gbadamosi, A.O., Agi, A., Ismail, A.R., Manoger, P., Ravichandran, K., 2020. Enhanced cuttings transport efficiency of water-based muds using (3–Aminopropyl) triethoxysilane on polypropylene-nanosilica composite. Arab. J. Chem. 13, 6904–6920. https://doi.org/10.1016/j.arabjc.2020.07.004.
Pakdaman, E., Osfouri, S., Azin, R., Niknam, K., Roohi, A., 2019. Improving the rheology, lubricity, and differential sticking properties of water-based drilling muds at high temperatures using hydrophilic Gilsonite nanoparticles. Colloids Surf. A Physicochem. Eng. Asp. 582,. https://doi.org/10.1016/j.colsurfa.2019.123930 123930.
Pan, Y., He, S., Gong, L., Cheng, X., Li, C., Li, Z., Liu, Z., Zhang, H., 2017. Low thermal-conductivity and high thermal stable silica aerogel based on MTMS/Water-glass co-precursor prepared by freeze drying. Mater. Des. 113, 246–253. https://doi.org/10.1016/j.matdes.2016.09.083.
Patidar, A.K., Ghosh, S., Thakur, N.K., Sharma, A., Baliyan, A., 2021. A review and comparative analysis of effectively functionalized eco-friendly and biodegradable nanoparticle based additives for drilling muds. Mater. Today:. Proc. 2021. https://doi.org/10.1016/j.matpr.2021.12.176.
Perumalsamy, J., Gupta, P., Sangwai, J.S., 2021. Performance evaluation of esters and graphene nanoparticles as an additives on the rheological and lubrication properties of water-based drilling mud. J. Pet. Sci. Eng. 204,. https://doi.org/10.1016/j.petrol.2021.108680 108680.
Piroozian, A., Ismail, I., Yaacob, Z., Babakhani, P., Ismail, A.S.I., 2012. Impact of drilling fluid viscosity, velocity and hole inclination on cuttings transport in horizontal and highly deviated wells. J. Pet. Explor. Prod. Technol. 2, 149–156. https://doi.org/10.1007/s13202-012-0031-0.
Prakash, V., Sharma, N., Bhattacharya, M., 2021. Effect of silica nano particles on the rheological and HTHP filtration properties of environment friendly additive in water-based drilling fluid. J. Pet. Explor. Prod. Technol. 11, 4253–4267.
Rafati, R., Smith, S.R., Sharifi Haddad, A., Novara, R., Hamidi, H., 2018. Effect of nanoparticles on the modifications of drilling fluids properties: a review of recent advances. J. Pet. Sci. Eng. 161, 61–76. https://doi.org/10.1016/j.petrol.2017.11.067.
Rahman, I.A., Padavettan, V., 2012. Synthesis of silica nanoparticles by sol-gel: size-dependent properties, surface modification, and applications in silica-polymer nanocomposites—A review. J. Nanomater. 2012, 1–15. https://doi.org/10.1155/2012/132424.
Rahman, I.A., Vejayakumaran, P., Sipaut, C.S., Ismail, J., Abu Bakar, M., Adnan, R., Chee, C.K., 2006. Effect of anion electrolytes on the formation of silica nanoparticles via the sol–gel process. Ceram. Int. 32, 691–699. https://doi.org/10.1016/j.ceramint.2005.05.004.
Rahman, I.A., Vejayakumaran, P., Sipaut, C.S., Ismail, J., Bakar, M. A., Adnan, R., Chee, C.K., 2007. An optimized sol–gel synthesis of stable primary equivalent silica particles. Colloids Surf. A Physicochem. Eng. Asp. 294, 102–110. https://doi.org/10.1016/j.colsurfa.2006.08.001.
Rahman, I.A., Vejayakumaran, P., Sipaut, C.S., Ismail, J., Chee, C.K., 2008. Effect of the drying techniques on the morphology of silica nanoparticles synthesized via sol–gel process. Ceram. Int. 34, 2059–2066.
Ramesh, K.T., 2009. Nanomaterials: Mechanics and mechanisms. Nanomater. Mech. Mech. 1–316. https://doi.org/10.1007/978-0-387-09783-1.
Rana, A., Arfaj, M.K., Saleh, T.A., 2020. Graphene grafted with glucopyranose as a shale swelling inhibitor in water-based drilling mud. Appl. Clay Sci. 199,. https://doi.org/10.1016/j.clay.2020.105806 105806.
Rezaei, A., Shadizadeh, S.R., 2021. State-of-the-art drilling fluid made of produced formation water for prevention of clay swelling: experimental Investigation. Chem. Eng. Res. Des. 170, 350–365. https://doi.org/10.1016/j.cherd.2021.04.012.
Rimer, J.D., Trofymluk, O., Navrotsky, A., Lobo, R.F., Vlachos, D. G., 2007. Kinetic and thermodynamic studies of silica nanoparticle dissolution. Chem. Mater. 19, 4189–4197. https://doi.org/10.1021/cm070708d.
Rowell, D.L., 2014. Soil science: Methods & applications. Routledge.
Sadegh Hassani, S., Amrollahi, A., Rashidi, A., Soleymani, M., Rayatdoost, S., 2016. The effect of nanoparticles on the heat transfer properties of drilling fluids. J. Pet. Sci. Eng. 146, 183–190. https://doi.org/10.1016/j.petrol.2016.04.009.
Sajjadian, M., Sajjadian, V.A., Rashidi, A., 2020. Experimental evaluation of nanomaterials to improve drilling fluid properties of water-based muds HP/HT applications. J. Pet. Sci. Eng. 190,. https://doi.org/10.1016/j.petrol.2020.107006 107006.
Saleh, T.A., Ibrahim, M.A., 2019. Advances in functionalized Nanoparticles based drilling inhibitors for oil production. Energy Rep. 5, 1293–1304. https://doi.org/10.1016/j.egyr.2019.06.002.
Saleh, T.A., Rana, A., Arfaj, M.K., Ibrahim, M.A., 2022. Hydrophobic polymer-modified nanosilica as effective shale inhibitor for water-based drilling mud. J. Pet. Sci. Eng. 209,. https://doi.org/10.1016/j.petrol.2021.109868 109868.
Salih, A.H., Elshehabi, T.A., Bilgesu, H.I., 2016. Impact of nanomaterials on the rheological and filtration properties of water-based drilling fluids. SPE East. Reg. Meet. 2016-Janua. 10.2118/184067-MS.
Schwanke, A.J., Pergher, S.B.C., 2013. Porous heterostructured clays - recent advances and challenges - revisão. Cerâmica 59, 576–587. https://doi.org/10.1590/S0366-69132013000400014.
Shakib, J.T., Kanani, V., Pourafshary, P., 2016. Nano-clays as additives for controlling filtration properties of water–bentonite suspensions. J. Pet. Sci. Eng. 138, 257–264. https://doi.org/10.1016/j.petrol.2015.11.018.
Shojaei, N., Ghazanfari, M.H., 2022. Reduction of formation damage in horizontal wellbores by application of nano-enhanced drilling fluids: experimental and modeling study. J. Pet. Sci. Eng. 210,. https://doi.org/10.1016/j.petrol.2021.110075 110075.
Singh, R., Tong, S., Panthi, K., Mohanty, K.K., 2018. Nanoparticle-encapsulated acids for stimulation of calcite-rich shales. SPE/AAPG/SEG Unconv. Resour. Technol. Conf. 2018, URTC 2018. 10.15530/urtec-2018-2897114.
Srivastava, V., Beg, M., Sharma, S., Kumar, A., Mud, B.M.B., Brunauer, B.E.T., Teller, E., Choubey, A.K., 2021. Application of manganese oxide nanoparticles synthesized via green route for improved performance of water-based drilling fluids. Appl. Nanosci. 11, 2247–2260. https://doi.org/10.1007/s13204-021-01956-8.
Srivatsa, J.T., Ziaja, M.B., 2011. An experimental investigation on use of nanoparticles as fluid loss additives in a surfactant - polymer based drilling fluid. Int. Pet. Technol. Conf. 2011, IPTC 2011.
Tadjarodi, A., Haghverdi, M., Mohammadi, V., 2012. Preparation and characterization of nano-porous silica aerogel from rice husk ash by drying at atmospheric pressure. Mater. Res. Bull. 47, 2584–2589. https://doi.org/10.1016/j.materresbull.2012.04.143.
Thuadaij, N., Nuntiya, A., 2008. Preparation of nanosilica powder from rice husk ash by precipitation method. Chiang Mai J. Sci. 35, 206–211.
Vasconcelos, D.C., Campos, W.R., Vasconcelos, V., Vasconcelos, W. L., 2002. Influence of process parameters on the morphological evolution and fractal dimension of sol–gel colloidal silica particles. Mater. Sci. Eng. A 334, 53–58. https://doi.org/10.1016/S0921-5093(01)01762-2.

Vryzas, Z., Mahmoud, O., Nasr-El-Din, H.A., Kelessidis, V.C., 2015. Development and testing of novel drilling fluids using Fe_2O_3 and SiO_2 nanoparticles for enhanced drilling operations. In: International Petroleum Technology Conference. International Petroleum Technology Conference.

William, J.K.M., Ponmani, S., Samuel, R., Nagarajan, R., Sangwai, J. S., 2014. Effect of CuO and ZnO nanofluids in xanthan gum on thermal, electrical and high pressure rheology of water-based drilling fluids. J. Pet. Sci. Eng. 117, 15–27. https://doi.org/10.1016/j.petrol.2014.03.005.

Xu, J., Qiu, Z., Zhao, X., Zhong, H., Li, G., Huang, W., 2018. Synthesis and characterization of shale stabilizer based on polyethylene glycol grafted nano-silica composite in water-based drilling fluids. J. Pet. Sci. Eng. 163, 371–377. https://doi.org/10.1016/j.petrol.2018.01.007.

Yang, X., Shang, Z., Liu, H., Cai, J., Jiang, G., 2017. Environmental-friendly salt water mud with nano-SiO2 in horizontal drilling for shale gas. J. Pet. Sci. Eng. 156, 408–418.

Zarei, V., Mirzaasadi, M., Davarpanah, A., Nasiri, A., Valizadeh, M., Hosseini, M.J.S., 2021. Environmental method for synthesizing amorphous silica oxide nanoparticles from a natural material. Processes 9, 334. https://doi.org/10.3390/pr9020334.

Zarei, V., Nasiri, A., 2021. Stabilizing Asmari Formation interlayer shales using water-based mud containing biogenic silica oxide nanoparticles synthesized. J. Nat. Gas Sci. Eng. 91,. https://doi.org/10.1016/j.jngse.2021.103928 103928.

Zarei, V., Emamzadeh, A., Nasiri, A., 2018. Synthesis of amorphous silica nanoparticles from natural materials applied in drilling fluid for stabilizing shale layers. J. Pet. Res. 27, 18–31. https://doi.org/10.22078/pr.2017.2683.2232.

Zhang, G., Dass, A., Rawashdeh, A.-M.-M., Thomas, J., Counsil, J. A., Sotiriou-Leventis, C., Fabrizio, E.F., Ilhan, F., Vassilaras, P., Scheiman, D.A., 2004. Isocyanate-crosslinked silica aerogel monoliths: preparation and characterization. J. Non Cryst. Solids 350, 152–164.

Zhao, X., Qiu, Z., Gao, J., Ren, X., Li, J., Huang, W., 2021. Mechanism and effect of nanoparticles on controlling fines migration in unconsolidated sandstone formations. SPE J. 26, 3819–3831.